

2024

Shear bond strength of different cements to printed resins and zirconia

<https://hdl.handle.net/2144/49521>

Downloaded from DSpace Repository, DSpace Institution's institutional repository

BOSTON UNIVERSITY
HENRY M. GOLDMAN SCHOOL OF DENTAL MEDICINE

Thesis

**SHEAR BOND STRENGTH OF DIFFERENT CEMENTS TO PRINTED RESINS
AND ZIRCONIA**

by

RAWAN TALEB ALLANQAWI

MChD, BChD, BSc University of Leeds, UK, 2016

CAGS in Prosthodontics, Boston University, 2023

Submitted in partial fulfillment of the requirements for the degree of

Master of Science in Dentistry

In the Department of Restorative Sciences and Biomaterials

2024

Approved by

First Reader

Russell A. Giordano II D.M.D., C.A.G.S., D.M.Sc.

Professor and Director, Division of Biomaterials

Department of Restorative Sciences and Biomaterials

Assistant Dean for Biomaterials & Biomaterials Research

Professor, Materials Science and Engineering

Second Reader

Yuwei Fan, BS, MSc, PhD

Research Associate Professor of Restorative Sciences and Biomaterials

Research Operations Director in Restorative Sciences and Biomaterials

Third Reader

Mohammad Dashti, D.M.D, C.A.G.S, FACP

Clinical Associate Professor

Division of Postdoctoral Prosthodontics

Department of Restorative Sciences and Biomaterials

DEDICATION

I would like to dedicate this work to my parents, my husband Mohammed, and my beautiful children Taibah and Yousef.

ACKNOWLEDGMENTS

I would like to express my sincere gratitude and appreciation to everyone who has contributed to the completion of this thesis. Your unwavering support, guidance, and encouragement have been helpful in shaping this research endeavor.

To my advisors, Dr. Fan Yuwei and Dr. Russell Giordano. Your mentorship has formed my research and nurtured my passion for learning. Your insightful feedback and constructive criticism have pushed me to new heights, and I am forever grateful for your guidance.

To my family, this endeavor would not have been possible without your support, patience, and encouragement. You have provided solace during challenging times and laughter during moments of celebration. I am truly humbled.

I am also thankful to the staff and administrators especially, Ms. Milly Koo. Your efficient coordination and helpfulness have significantly contributed to the smooth progress of this thesis.

**SHEAR BOND STRENGTH OF DIFFERENT CEMENTS TO PRINTED RESINS
AND ZIRCONIA**

RAWAN ALLANQAWI

Boston University, Henry M. Goldman School of Dental Medicine, 2024

Major Professor: Russell Giordano II, D.M.D., D.M.Sc., Director, and Associate

Professor

Department of Restorative Sciences and Biomaterials

ABSTRACT

Objectives: This in-vitro study aimed to measure bonding of multi and single step cements to printed resins and Layzir zirconia. Evaluate the effect of different material combinations on shear bond strength, and to evaluate the effect of thermocycling on shear bond strength of different materials combinations.

Materials and Methods:

Rectangular specimens (N= 384) were prepared from PacDent Rodin Sculpture 2.0 (RS), SprintRay Ceramic Crown (SCC), Rodin Titan (RT), and Layzir Zirconia (LZ), and were divided into 16 groups according to material combinations, static or thermal aging process. Stainless-steel rods (Shofu Dental Corporation) of 4 mm diameter were used for this in-vitro study. Shear bond strength (SBS) test was performed on all static and thermocycled groups. The final dimension of each plate was about 15 mm in length, 2mm thick, and 15 mm in width. 3D printing of resins was done using the Asiga 3D printer. Layzir Zirconia specimens were prepared by sectioning the zirconia disc using the Isomet 5000 sectioning machine. Zirconia specimens were dried in the oven and sintered using a high temperature

furnace (Zircar). All materials were surface treated based on material recommendations. All stainless-steel rods and Layzir Zirconia were sandblasted, PacDent Rodin Sculpture 2.0 and Rodin Titan were etched with hydrofluoric acid 5%, and SprintRay Ceramic Crown was sandblasted and etched using 5% Hydrofluoric acid. In the last stage of specimen preparation, the framework plate was placed on a flat surface, then the adhesive resin cement was injected to fill the bonding area. Excess cement was removed around the rod border with a plastic instrument and a micro brush, and the bonded plate/rod was kept under a static load of 1.4 kg for 10 minutes. Half of the specimens were tested in a control/static condition, and another half were thermal aged for 5000 cycles before shear bond testing was done. A shear bond test was performed on all static and thermocycled specimens by using the universal testing machine (Instron Model 5566A). The crown material was secured into a jig and a flat shear blade was used to shear the pins. The blade had a perpendicular contact at the interface between the rod and the plate. A load was applied at the adhesive interface between the plate/rod during the testing. The shear bond strength was calculated in MPa by load of failure over the area of the bond. The maximum shear load was recorded at debonding. Specimens were examined to determine failure location, load to failures values were also analyzed as well as the mode of failures.

Results:

This study showed a significant difference in shear bond strength between the printed resin groups compared to Layzir Zirconia group ($P < .0002$). Layzir Zirconia group showed the lowest SBS mean values among the tested groups (16.18 MPa). SprintRay bonded with Panavia SA materials produced the highest shear bond strength mean values (32.07MPa),

followed by Rodin Titan bonded with Panavia V5 and Clearfil (30.91MPa) and Panavia SA (29.50 MPa), and PacDent Rodin Sculpture 2.0 Bonded with Panavia SA (25.51 MPa). The lowest shear bond strength mean values were recorded in SprintRay bonded with Clearfil and Panavia V5 (17.26 MPa), Layzir Zirconia bonded with Rodin bond and Panavia V5 (15.06 MPa), and Pacdent Sculpture 2 bonded with Clearfil and Panavia V5 (13.62 MPa). There was a significant difference in SBS between control and treated (thermal cycle) groups (decrease in treated group than control group) ($P<.0001$). There's a significant difference between SBS values for specimens bonded with Panavia SA compared to other resin cements used ($P<.0001$).

Conclusion: Significant differences were found between 3D printed resins compared to Layzir Zirconia groups. Layzir Zirconia groups showed the lowest SBS among all tested groups. Thermal aging significantly decreased SBS values of thermocycled groups. Adhesive failure was the primary mode of failure among all SBS tested groups. Material surface topography, filler content, surface pretreatment and adhesive techniques, as well as thermal aging impact the bonding and as a result SBS values of specimens.

TABLE OF CONTENTS

APPROVED BY	ii
DEDICATION	iii
ACKNOWLEDGMENTS	iv
ABSTRACT	v
TABLE OF CONTENTS.....	viii
LIST OF TABLES	xi
LIST OF FIGURES	xiii
LIST OF ABBREVIATIONS.....	xvi
CHAPTER 1. INTRODUCTION	1
1.1 Digital Dentistry	1
1.2 Types of 3D printers (differences and limitations).....	3
1.2.1 Stereolithography (SLA).....	4
1.2.2 Digital Light Processing (DLP).....	4
1.2.3 Liquid Crystal Display (LCD)	5
1.3 Shear bond test overview	5
1.4 Overview of CAD/CAM and printed resins	6
1.4.1 PacDent Rodin Sculpture 2.0.....	6
1.4.2 Rodin Titan	7
1.4.3 SprintRay Ceramic Crown.....	7
1.4.4 Layzir Zirconia.....	7
1.5 Overview of zirconia	8

1.6 Overview of cements	9
1.6.1 Types of cements	10
1.7 Single and multi-step bottle adhesives.....	13
1.7.1 Single step adhesive systems	13
1.7.2 Multi step adhesive systems.....	14
1.8 Bonding to materials (Resin and zirconia)	14
1.9 Surface treatments of zirconia and resins (acid etching and sandblasting)	16
1.9.1 Airborne-particle abrasion (APA) with alumina particles	18
1.9.2 Hydrofluoric Acid (HF) Etching.....	20
1.10 Mechanical properties.....	20
1.12 Objectives	22
1.13 Null hypothesis	23
CHAPTER 2. MATERIALS & METHODS	24
2.1 Materials	24
2.2 Equipment:.....	30
2.3 Methods:	33
2.3.1 Material preparation.....	33
2.3.2 Surface preparation	35
2.3.3 Cementing process.....	37
2.4 Thermocycling.....	39
2.5 Shear Bond testing	39
2.6 Failure mode analysis using digital microscope	40

2.7 Statistical Analysis:.....	43
CHAPTER 3. RESULTS	44
3.1 Shear bond test results	44
3.1.1 SBS affected by different material.....	49
3.1.2 SBS affected by cement-bond.....	50
3.1.3 SBS affected by post-treatment.	51
3.1.4 SBS affected by material and cement-bond system interaction.....	52
3.1.5 SBS affected by material and post-treatment interaction.	54
3.1.6 SBS affected by cement-bond and post-treatment interaction.....	56
3.2 Mode of failure	57
3.3 Correlation of failure mode and shear bond strength	63
CHAPTER 4. DISCUSSION.....	67
4.1 Shear bond strength	67
4.2 Limitations of this study	72
4.3 Recommendations for Future Studies.....	73
CHAPTER 5. CONCLUSION	75
CHAPTER 6. REFERENCES	76
CURRICULUM VITAE.....	76

LIST OF TABLES

Table 1: Summary of mechanical properties of materials used in this study	20
Table 2. Characteristics of cements used in the study	27
Table 3. Characteristics of Adhesives/primers used in the study	28
Table 4. Surface treatment for all materials prior to bonding.....	36
Table 5. Material-cement-bond combination.....	41
Table 6. SBS and mode of failure of different cement and material combinations.....	45
Table 7. Effect summary of material, cement-bond, and post-treatment on SBS	47
Table 8. connecting letters report for comparing different group materials on SBS values among all groups using Tukey-Kramer HSD	49
Table 9. Connecting letters report for comparing different cements on SBS values among all groups using Tukey-Kramer HSD	51
Table 10. Summary of mean of control and thermocycled groups.....	52
Table 11. Connecting letters report for comparing different materials and cement-bond on SBS values using Tukey-Kramer HSD.....	53
Table 12. Connecting letters report for comparing different materials on SBS values among all groups (control and thermocycled) using Tukey-Kramer HSD.....	55
Table 13. Connecting letters report for comparing different cements on SBS values among all groups (control and thermocycled) using Tukey-Kramer HSD.....	56
Table 14. Mode of failure among all cement+bond groups.....	58
Table 15. Table of failure mode between control and treated (thermocycled) SBS groups	60

Table 16. Mode of failure among all tested SBS groups	61
Table 17. One-way Anova and Tukey HSD test of SBS and mode of failure.....	63
Table 18. Connecting letters report for comparing SBS mean values and mode of failure using Tukey-Kramer HSD	64

LIST OF FIGURES

Figure 1. Materials used in the study. A) Pacdent Sculpture 2.0 B) SprintRay Ceramic Crown, C) Rodin Titan, and D) Layzir Zirconia	24
Figure 2. Panavia SA cement used in the study.....	25
Figure 3. Panavia V5 cement used in the study.....	25
Figure 4. Resicem Ex cement used in the study	25
Figure 5. HC primer used in the study	26
Figure 6A. AZ primer used in the study	26
Figure 7. stainless-steel rods used in the study.....	29
Figure 8. Left Aiga 3D printer used in the study. Right Otoflash G171.....	30
Figure 9. Instron 5566A Universal Testing Machine	30
Figure 10. BUEHLER Isomet-5000 precision saw.....	31
Figure 11. Thermocycling test apparatus.....	31
Figure 12. Sandblaster: Renfert Basic Quattro	31
Figure 13. Fisher Scientific Oven (Thermo scientific, OH, USA)	32
Figure 14. Sintering oven: Hot spot 110 lab furnace.....	32
Figure 15. Layzir Zirconia specimen preparation. A) Disc sectioned into blocks, then blocks into plates. B) Prepared specimens were sintered in Zircar furnace.	34
Figure 16. Recommended sinter program.....	35
Figure 17. Top: Before and after bonding framework plate and rod. Bottom: All framework plates and veneer rods were bonded; excess cement was removed and	

bonded. The specimens were kept under a static load of 1393 g (1.4 kg/13.66N) for 10 minutes in a cylindrical loading apparatus.....	38
Figure 18. Specimens were placed in the shear bond test fixture. A flat/knife edge blade was used to shear the rods.....	40
Figure 19. Keyence Digital Microscope	40
Figure 20. Actual whole model of SBS of all groups by predicted plot ($R^2=0.49$, P- value<0.0001)	47
Figure 21. SBS least square mean plot affected by different material combinations.	49
Figure 22. SBS least square mean plot affected by cement-bond combination.....	Error!
Bookmark not defined.	
Figure 23. SBS least square mean plot between control and post-treatment groups .	Error!
Bookmark not defined.	
Figure 24. Graphic illustration of mean shear bond strength of the tested groups	53
Figure 25. SBS least square mean plot between control and post-treatment groups	55
Figure 26. SBS least square mean plot affected by cement-bond combination in control and thermocycled group combinations	56
Figure 27. Mode of failures for SBS (Source: Instron, ASTM D1002 Lap Shear Testing of Adhesively Bonded Materials)	58
Figure 28. Mosaic plot of failure mode affected by cement-bond combination.....	59
Figure 29. Mosaic plot of failure mode by post-treatment	60
Figure 30. Mosaic plot of failure mode affected by substrate material	62

Figure 31. One-way analysis of shear bond strength MPa by mode of failure (adhesive, cohesive, mixed failure).....	63
Figure 32. Adhesive failures shown in the failed SBS specimens.....	65
Figure 33. Cohesive and mixed failures among groups.....	65
Figure 34. Adhesive failures shown in the failed SBS specimen (Layzir Zirconia, Rodin Bond, Panavia V5).....	66
Figure 35. cohesive failure shown in the failed SBS specimen (Pacdent, Rodin Bond, Panavia V5).....	66

LIST OF ABBREVIATIONS

ADA	American Dental Association
Al ₂ O ₃	Aluminum oxide
ANOVA	Analysis of variance
APA	Airborne-particle abrasion
ATZ	Alumina Toughened Zirconia
Bis-GMA	Bisphenol A diglycidylmethacrylate
CAD-CAM	Computer-aided design & Computer-aided manufacturing
CAM	Computer-aided manufacturing
CDT	Code on Nomenclature
CTE	Coefficient of thermal expansion
CV	Coefficient of variance
FDA	Food and drug Administration
FDP	Fixed dental prosthesis
FPDs	Fixed partial dentures
FS	Fully sintered
GIC	Glass ionomer cement
HEMA	Hydroxy methacrylate
HF	Hydrofluoric Acid
HfO ₂	Hafnium oxide

HPMC	Hydroxypropyl Methylcellulose
IPA	Isopropyl alcohol
ISO	International standards organization
kg	Kilogram
LCD	Liquid crystal display
LED	Light emitting diode
MDP	10-Methacryloyloxydecyl dihydrogen phosphate
Min	Minute
MPa	Megapascal unit
n	Number of samples per group
N	Newton unit (force)
Na ₂ O	Sodium oxide
P Value	Probability Value
P-SA	Panavia SA Universal cement
P-V5	Panavia V5 cement
PC	Polycarboxylate cement
PFM	Porcelain-fused-to-metal
PMMA	Polymethylmethacrylate
PS	Partially sintered
PSZ	Partially stabilized zirconia
RS	PacDent Rodin Sculpture
RT	Rodin Titan

SBS	Shear bond strength
SCC	Sprintray ceramic crown
SD	Standard deviation
SiO ₂	Silicon dioxide
TC	Thermal Cycling
TEGDMA	Triethylene glycol dimethacrylate
TZP	Tetragonal Zirconia Polycrystal
UDMA	Urethane Dimethacrylate
wt%	Percentage by weight
Y-TZP	Yttria-stabilized Tetragonal Zirconia Polycrystal ceramics
ZPC	Zinc phosphate cement
ZrO ₂	Zirconium dioxide

CHAPTER 1. INTRODUCTION

1.1 Digital Dentistry

3D printing of various dental prosthetic devices such as dentures, surgical guides, mouthguards, and provisional restorations has been increasing over the past 5 years. Prior to 2022, ceramic was defined by the American Dental Association as: “pressed, fired, polished or milled materials containing predominantly inorganic refractory compounds including porcelains, glasses, ceramics, and glass-ceramics.”. The new definition eliminates “pressed, fired, polished or milled materials”. The deletion of the manufacturing criteria from the definition of porcelain/ceramic opens the door to permanent restorations printed with predominantly inorganic refractory compounds (American Dental Association, 2022).

In the fall of 2022, the ADA changed the definition of a ceramic restoration to include “printed materials with predominantly a ceramic or glass filler”.

Since that time, many materials have been introduced for clinical use with little or no in vitro or in vivo research.

The field of dentistry has advanced significantly from the integration of technology, providing more cost-effective treatments that prioritize the performance of dental prosthetics. Recent software technology, such as intraoral scanners, cameras, and lasers, can transfer data for fabricating custom dental restorations using subtractive and additive techniques. With the assistance of computer-aided design (CAD) software, the data can be accurately analyzed to create a 3D model. Computer-aided manufacturing (CAM) software then sends the design to milling or 3D printing machines to fabricate dental prosthetics.

Developments in material composition and mechanical properties made the CAD/CAM workflow more efficient, resulting in a more streamlined and reliable process.

Implementing Subtractive (milling) method of CAD/CAM offers various benefits to the practice. In comparison to the conventional method, using a digital scan with a milling machine eliminates the need for conventional impressions, diagnostic cast, wax-ups, investing, casting, and firing (Davidowitz, 2011). Milling machines provide same-day permanent restoration, which is more convenient for patients as there is no need for additional visits or need to fabricate provisional prosthesis. According to Turkeyilmaz (2021) stated that multi-axis milling machines improve fabricated prosthesis accuracy and speed. While the accuracy of the prosthesis is affected by the wear of milling burs and the limitation of the bur's path (Moon, 2022). Involving ceramic materials improve aesthetics, translucency with various shades and advanced mechanical properties. One drawback of the milling machine is the initial investment in the system, which can counterweigh for the additional cost of the outside laboratory over time.

Three-Dimensional printing or additive manufacturing is adding material in layers to fabricate objects designed by CAD software (Huang, 2013). The object must be in the Standard Transformation Language (STL) file format. CAM software slices virtual models into horizontal layers, representing the x and y-axis. Layer thickness is associated with the object resolution and represents the z-axis. As layer thickness get smaller, it increases the object's smoothness and more time to print (Kessler, 2020). There is innovative growth in the use of 3D printing in dentistry because of the capability of customization that improves patient care. The accuracy of 3D printing is affected by laser speed, laser intensity, build

orientation, support structure configuration, layer thickness, type of 3D printer, post-processing protocol, and type of material (Nulty, 2022) (Ko, 2021) (Tian Y. C., 2021) (Hartley, 2022) (Jockusch, 2020) (Dong, 2020).

1.2 Types of 3D printers (differences and limitations)

In the dental field, there are diverse technologies available for 3D printing. These include fused deposition modeling (FDM) and fused filament fabrication (FFF), where a heated nozzle melts and extrudes thermoplastic filaments in layers. Material jetting uses droplet of liquid polymer to print objects in different colors and materials. Selective laser sintering (SLS) utilizes lasers or electron beams to fuse powder grains together for powder bed fusion technology, while vat polymerization selectively cures liquid polymer with ultraviolet light to form solid layers. It is important to consider specific requirements when choosing a 3D printing method for dental applications, as each technology has advantages and disadvantages (Schweiger, 2021).

The most common 3D printer polymerization technology for polymers in the market: stereolithography (SLA), digital light processing (DLP), and Liquid Crystal Display (LCD). These technologies focus on a light source in specific wavelength irradiation to cure and polymerize resin in a liquid state of addition layer by layer to print the whole model (Bagheri, 2019). 3D printers with the same technology have different resolutions because of the differences in the wavelength, power, and exposure time for each material (Jockusch, 2020).

1.2.1 Stereolithography (SLA)

SLA method uses an ultraviolet (UV) laser to activate the photopolymerization of resin and print layer sequentially with a distance equal to layer thickness. Motorized mirrors are used to focus the laser beam through a resin vat to move the X and Y dimension of the beam. While Z-axis controls the movement of the build platform vertically depending on the layer thickness (Javaid, 2019). The laser beam consolidates resin in layers and connects them in the Z-axis. The wavelength strength of the laser and exposure time influence the curing of resin (Stansbury, 2016). SLA technology has temperature resistance, the ability to print complex shape objects with a support structure, high accuracy, and more time to print and post-processing (Abduo, 2014) (Turkyilmaz, 2021).

1.2.2 Digital Light Processing (DLP)

DLP technology uses digital projectors with an arrangement of micromirrors, each representing one pixel or more of the CAD model per layer (Revilla-León, 2019). This digital projector cures the entire layer in the x-y axis at one reflection of UV irradiation, which gives it the advantage of speed. The resolution of the projected reflection depends on the number and the adjustment angle of mirrors (Tian Y. C., 2021). One drawback of DLP is that it produces voxel lines that make steps that affect the smoothness of curve shape objects that need polishing in the postprocessing step. Nevertheless, DLP printers print high-precision finer objects, have fast printing speed, and smooth surfaces (Zhu, 2022).

1.2.3 Liquid Crystal Display (LCD)

LCD 3D printer (Masked stereolithography) is an innovative technology that combines DLP and stereolithography technology. It functions similarly to a DLP printer, as the whole resin layer is photopolymerized at once, layer per layer, until the print is complete. However, LCD printers utilize an array of UV LEDs to cross-section images of layers and block out the remaining field of the back panel (Chen, 2021) (Sotov, 2021). The advantage of eliminating the motorized mirrors or digital projectors in SLA and DLP printers makes it more affordable. On the other hand, the life span of LCD depends on the LCD screens as they need to be replaced more than DLP. The precision of LCD is lower than DLP because of the Partial light leakage that happens through the molecular arrangement of the LCD panels (Quan, 2020) (Tsolakis, 2022).

1.3 Shear bond test overview

As part of dental research, adherence assessment is accomplished effectively only by bond strength testing (Ilie and Ruse, 2019). Two materials are joined by an adhesive agent in a shear bond test, then loaded in shear before fracture occurs (Sirisha, 2014).

Because of their simplification, the shear bond strength test remains one of the most common and versatile method used versus the tensile bond strength tests (Placedo et al, 2007). The advantages of shear testing include ease of handling of specimens and a standard test protocol (Placedo et al, 2007). A meta-analysis including its factors involved in bond strength testing exhibited the major impact of different parameters, including such

dentin substratum, composite and bonding area, bond storage and test design conditions (Sirisha, 2014).

Even though selected studies state that the bonding surpassed the substrate's cohesive strength without necessity for additional enhancement, the correct explanation here is that this test proved inappropriate for determining the appropriate strength of a bonded interface. The actual rationale for this fact, according to Della Bona and van Noort, was that stresses were contained more in the substrate, leading to its premature failure before the interface itself (Placido et al, 2007).

1.4 Overview of CAD/CAM and printed resins

Asiga 3D printers use an exclusive Smart Positioning System (SPS) technology to manufacture accurate and repeatable prints. SPS uses pressure sensors to sense the position of the build platform and the viscosity of the resin after each layer is cured. This permits the printer to settle between layers and guarantee that each layer is the correct thickness before curing. SPS also aids in preventing deflection and analyzes layer formation to ensure proper layer thickness.

1.4.1 PacDent Rodin Sculpture 2.0

This material is a zirconia filled nanohybrid resin that achieves high flexural strength and ceramic filler content values, allowing the material to provide wear and fracture resistance. PacDent Rodin Sculpture 2.0 is FDA 510(K) cleared and fulfilled all

requirements for class II medical device. Sculpture 2.0 has a filler content to over 60% and a biaxial flexural strength of over 200 MPa.

1.4.2 Rodin Titan

This material is a ceramic nanohybrid resin engineered for the printing of full arch restorations and provisional hybrid dentures. Rodin Titan is FDA 510(K) cleared (K240688) and fulfilled all requirements for class II medical device. Rodin Titan has a modified flexural modulus to tailor printing full arch restorations and provisional hybrid dentures (PacDent, 2023).

1.4.3 SprintRay Ceramic Crown

This material is a hybrid nanoceramic that is FDA-cleared for permanent restoration of crowns, partial crowns, and veneers. SprintRay Ceramic Crown is described as having high mechanical properties (Ceramic Crown Brochure, 2023). It is exclusively compatible with SprintRay ecosystem printers and curing machines. It has more than 50% weight of inorganic content.).

1.4.4 Layzir Zirconia

This is a multi-layer zirconium dioxide with 3Y-TZP forming the “cervical” layer and 5Y-PSZ forming the “occlusal” layer used for manufacturing fixed dental prostheses. The manufacturer reports a flexural strength of 1,450 MPa at the cervical layer and 1,030 MPa at the occlusal layer (Smart Dentistry Solutions, 2024).

1.5 Overview of zirconia

The literature recognizes zirconia ceramic material as suggestions for both single and fixed dental prostheses (FDP) fabrication. Various studies have presented that ceramics based on zirconia have superior mechanical strength compared to lithium disilicates and leucite containing feldspar. (Miyazaki, 2013) (Cassuci,2011).

Zirconia restorations are usually made with a partially sintered green body that is sintered to full density and as such requires a geometric size increase of up to 20-30 per cent by means of subtractive computing-assisted design/computing-aided (CAD/CAM) technology. Subtractive construction can be accomplished either using carbide burs milling technology or using diamond-coated instruments with grinding technology. In dry and wet environments, all processing methods can be accomplished. The majority of today's zirconia restorations are fabricated using CAM dry-milling construction procedures (Zimmermann, 2020).

There are three crystallographic forms of zirconia: monoclinic from room temperature to 1170 °C, tetragonal from 1170 °C to 2370 °C and cubic from 2370 °C to the point of melting (Miyazaki, 2013). The addition of about 3 mol% yttria produces a partially stabilized tetragonal zirconia. As more yttria is added the cubic content increases (Li, et al, 2014).

There is a significant demand for restorations that are nonmetallic, and biocompatible. As a result, ceramics have found widespread application in dentistry due to their capability to deliver highly esthetic results that closely resemble natural teeth.

Furthermore, they exhibit satisfactory mechanical strength when exposed to the forces of mastication. The rapid development in ceramic materials and manufacturing procedures has made it possible to treat both anterior and posterior teeth, aspiring to restore their form, function, and esthetic appearance without the use of metal components.

Zirconia, also known as zirconium dioxide (ZrO_2), is a crystalline oxide of the metal zirconium. It is a ceramic material that retains excellent mechanical, thermal, and chemical properties, making it beneficial in several applications. Zirconia is recognized for its high strength, hardness, and wear resistance. It is a high-performance ceramic material that has transformed the field of restorative dentistry. Due to its biocompatibility and tooth-colored appearance, zirconia is normally used as a dental material for crowns, bridges, and implants. It offers greater esthetics and durability related to traditional materials as metal or porcelain.

1.6 Overview of cements

Dental luting agents are required to retain restorations, appliances, and posts and cores in the oral environment, intending for long-lasting stability. The main techniques of retention and bonding using dental cements include mechanical interlocking, chemical bonding, and micromechanical retention. In the field of biomaterials, bonding strength is the measure of the load required to fracture a bond, divided by the cross-sectional area of the bond. This can be assessed via shear, tension, or pull-out tests. Some materials demonstrate adhesive properties, permitting them to bond two surfaces together, while

others may bond to one surface and create mechanical interlocking with the second surface (McCabe, 2007).

1.6.1 Types of cements

Various types of cements can be used in dentistry. These cements must have certain characteristics to guarantee acceptable clinical performance. This involves satisfactory resistance to dissolution, strong bonding through mechanical interlocking and adhesion, high tensile strength, favorable manipulation properties, and biocompatibility with the substrate (Meyer et al, 1998) (Rosenstiel et al, 1998). Two main types of dental luting cements are available: conventional non-resin-based types of cement and resin-based composite types of cement.

1.6.1.1 Conventional Non-Resin Cement

Conventional cement involves zinc phosphate cement (ZPC), polycarboxylate cement (PC), and glass ionomer cement (GIC). The retention of traditionally cemented indirect restorations is predominantly determined by frictional forces between the preparation's walls and the internal walls of the restoration. Thus, it is fundamental to prepare macro-retentive tooth preparation along with an accurate marginal fit (Edelhoff and Ozcan, 2007).

1.6.1.2 Glass ionomer cement

Glass ionomer cements have benefits such as physicochemical bonding to tooth structures, longstanding fluoride release, and low coefficients of thermal expansion. GICs

are comprised of a calcium or strontium aluminosilicate glass powder and a water-soluble polymer, typically polyacrylic acid. It is biocompatible, has the advantage of fluoride release, chemically bond to enamel and dentin, and has coefficient of thermal expansion similar to natural tooth structure. Nonetheless, their low mechanical strength limits their use in high-stress-bearing parts. Glass ionomer cements are used to cement core-reinforced ceramics harmonious with zinc phosphate, but they may not offer adequate support for ceramics demanding strong cement adhesion (Edelhoff and Ozcan, 2007).

1.6.1.3 Resin cement

The introduction of resin-based cement has transformed the field of dentistry, altering the primary principles of dental applications. Resin-based types of cement have grown in popularity because of their ability to address the shortcomings of solubility, support, and adhesion associated with conventional materials (Meyer et al, 1998).

In the past, the durability and lifespan of cemented restorations relied greatly on the geometry of the preparation, encompassing resistance and retention principles. Conversely, with the introduction of resin types of cement, the choice of restorative materials became more independent of geometric considerations. Hence, resin types of cement have ushered in a new period of treatment possibilities, proposing extended options for a larger range of clinical situations (Terry, 2004).

Resin composite cement involves three main components: an organic resin matrix, an inorganic filler, and an interphase that bonds the resin matrix and fillers that is a coupling agent (Sümer and Deger, 2011). The above components have a critical role in shaping the properties and performance of the resin composite. Physical properties for example,

strength, stiffness, thermal expansion coefficient and abrasion resistance are affected by the coupling agent and the filler, on the other hand, degradation and color stability are influenced by the resin matrix (Asmussen, 1984).

Resin composite cement possess various advantages in comparison to other dental cements, such as high bonding strength, compressive strength, tensile strength, and low solubility. The efficiency of resin cement relies on multiple factors regarding the bonding mechanisms between dental tissues and restorations (Ha, 2015). Originally, resin-based luting types of cement were mainly prepared using acrylic resin chemistry but, their advancement has been affected by the chemistry of resin composites and adhesives (Christensen, 1993). Currently, two main classifications of resin composite cements are available; first type is conventional resin cement that requires the use of a separate bonding agent (Segarra, 2015) (Jongsma, 2012) (Radovic et al, 2008). These cements are technique sensitive and are subjected to handling errors (Segarra, 2015). The second classification is self-adhesive resin cement that disregards the demand for a separate bonding treatment on the dental substrate as their acid-functionalized monomers can demineralize and infiltrate enamel and dentin (Ferracane, 2011) (Radovic et al, 2008).

Three mechanism of resin cements curing are available: chemical, visible light, and both chemical and light (dual cure). The majority of the resin types of cement available in the market are dual cured.

Studies have presented that the choice of cement type can influence stress distribution in monolithic zirconia crowns. Resin cement exhibited better stress distribution in comparison to zinc phosphate cement, polycarboxylate cement, and glass ionomer

cement (Ha, 2015). Ha (2015) stated that resin types of cement offered better retention than zinc phosphate cement or glass ionomer cement.

1.7 Single and multi-step bottle adhesives

The development of adhesive materials has begun to revolutionize many aspects of restorative dentistry. Attitudes towards cavity preparation are altering since, with adhesive materials, it is no longer necessary to prepare the cavity to provide mechanical retention through such features as dovetails, grooves, undercuts, sharp internal angles in order to retain the filling (Sofan et al, 2017). These techniques are, therefore, responsible for the conservation of large quantities of sound tooth substance, which would otherwise be victim to the dental bur. Microleakage which is probably responsible for many cases of secondary caries, may be reduced or eliminated (Vaidyanathan and Vaidyanathan, 2009). These adhesives are therefore critical for the success of aesthetic restorative materials in modern dentistry.

1.7.1 Single step adhesive systems

These systems are also called self-etch, they combine etching, priming, and bonding into one application step. Self-etching systems were introduced to control the sensitivity to humidity of the etch-and-rinse technique as well as to simplify the clinical procedures of the adhesive application, reducing clinical time and over-etching (Sundfeld, 2005). The self-etch adhesive systems are classified based on the number of clinical application steps: two-steps or one-step adhesives (Sundfeld, 2005) (Meerbeek, 2005).

1.7.2 Multi step adhesive systems

Adhesives that include a phosphoric acid-etching step are known as etch-and-rinse (ER) adhesives or multi bottle adhesives. They dissolve and remove the smear layer and smear plugs. This adhesive system includes steps for etching, priming, and bonding. It can either be a three step or two step adhesive system. Adhesives that do not use a separate etching step are known as self-etch (SE) adhesives, as they do not remove the smear layer, but are incorporated into the adhesive interface (Perdigão, 2020).

1.8 Bonding to materials (Resin and zirconia)

Adhesive bonding techniques and modern all-ceramic systems provide an extensive variety of highly esthetic treatment options. Bonding to traditional silica-based ceramics is a predictable procedure providing durable results when guidelines are followed. But, the composition and physical properties of high strength ceramic materials, like aluminum oxide-based (Al_2O_3) and zirconium oxide-based (ZrO_2) ceramics vary significantly from silica-based ceramics and necessitate alternative bonding techniques to provide a strong, long-term, durable resin bond (Blatz et al, 2003).

Resin-based composites are considered the material of choice for the adhesive luting of ceramic restorations. Composite cements possess compositions and characteristics comparable to conventional restorative composites and consist of inorganic fillers embedded in an organic matrix (for example: Bis-GMA, TEGDMA, UDMA). Composite cements are categorized in their initiation mode as auto-polymerizing (chemically activated), photoactivated, or dual-activated materials (Blatz, 2003).

Photoactivated composites provide great ranges of shades, consistencies, and compositions. Clinical application is simplified throughout extended handling times before and rapid hardening after exposure to light, shade, thickness, and transmission coefficient of the bonded ceramic restoration and the composite itself affect the conversion rate of the photo-activated material and constrain its application to thin silica-based ceramics (Blatz, 2003).

Dual-activated composites provide prolonged working times and controlled polymerization, although chemical activators guarantee a high degree of polymerization. The majority of dual-activated resin cements necessitate photopolymerization and exhibited inferior hardness when light polymerization was omitted. Numerous dual activated resin cements revealed no differences in resin-bond strengths between glass ceramics and enamel. Auto polymerizing resin cements have fixed setting times and are generally designated for resin bonding metal-based or opaque, high-strength ceramic restorations (Blatz, et al, 2003).

Self-adhesive resin cements were made according to the chemistry of resin cements and self-etch adhesives. They etch, prime, and bond to dentin without the need for separate agents for each step. Hence, the application is simple, and the idea of the smear layer as a bonding substrate has been reinstated with the anticipation of a low occurrence of postoperative sensitivity and pulp response (Blatz et al, 2003).

Their application can be done in a single clinical step, like cementation processes with conventional luting agents. In addition to the simplified application techniques, they

appear to be less prone to moisture contamination. A low incidence of postoperative sensitivity is expected with these luting agents (Perdigão, 2020).

According to these qualities and widespread applications, these cements have become widespread in clinical use.

1.9 Surface treatments of zirconia and resins (acid etching and sandblasting)

Mechanical and chemical retention are mandatory to provide a strong bond between a resin and a ceramic. Numerous surface treatments for resin bonding to zirconia have been suggested including sandblasting, tribochemical silica coating, hydrofluoric acid, and laser irradiation. But, as a result of high crystalline content and lack of a glass phase, hydrofluoric acid etching does not lead to a satisfactory resin bond to zirconia (Altan et al, 2019).

Sandblasting offers a rough surface for mechanical retention. Concurrently, sandblasting increases the strength of the Y-TZP and can compromise the compressive stress layer and lead to propagation of cracks (Altan et al, 2019). Up to the present time, the suggested bonding technique to zirconia frameworks is the mixture of sandblasting and 10-MDP monomer-based resin. However, the result of this procedure can vary due to factors such as particle size and application distance. Especially, excessive particle size and reduced sandblasting distance will lead to the development of cracks, and in turn decreasing ceramics' mechanical properties in the long term (Casucci et al, 2011).

The incorporation of functional monomers in dental adhesive systems promotes chemical interaction with dental substrates, resulting in higher adhesion forces when

compared to micromechanical adhesion only. Recently, zirconia primers were introduced to chemically bond to zirconia and to strengthen the resin-zirconia bond.

Resin types of cement and primers containing 10-methacryloyloxy-decyl dihydrogen phosphate (10-MDP) monomer have been considered the materials of choice because of the chemical interaction established between the hydroxyl groups of the zirconia ceramic and the phosphate ester monomer of the MDP-containing material (Oyaguyue et al, 2009)(Tanaka et al, 2008). The chemical structure of 10-MDP monomer allows for a polar behavior favorable to adhesion and promotes the protection of collagen fibers through the formation of MDP-calcium salts. Resin luting types of cement such as Panavia (Blatz et al, 2004), and some primers such as Alloy Primer, and Clearfil ceramic primer plus (Kuraray, Osaka, Japan) are representatives of this type of material.

Inokoshi et al (2014) meta-analysis stated that a mixture of mechanical and chemical pretreatments seemed to be essential for lasting bonding, however cement selection was not disclosed as a determining factor as long as a composite luting cement was used.

Surface treatment is recommended for proper adhesion between the dental cement and the inner surface of the zirconia (Ozcan and Vallittu, 2003) (Ozcan, 2002). It can be divided into micromechanical and chemical treatment. It has been found through in vitro studies and systematic reviews that a combination of micromechanical and chemical treatment is essential to attain long-term durable resin bonds (Blatz et al, 2007) (Koizumi et al, 2012) (Inokoshi et al, 2014).

Zirconia ceramic has a polycrystalline structure, which is acid resistant (Blatz et al, 2003) (Thompson et al, 2011). For cementation, silica-based ceramics are etched to achieve decent bonding using hydrofluoric acid, followed by saline application. On the other hand, zirconia is a silica-free ceramic and is unaffected by conventional etching procedures (Blatz et al, 2003) (Thompson et al, 2011). Surface treatments for example air abrasion with aluminum oxide particles coarsen the zirconia surface and increase the bond strength (Yun, 2010). Additional surface treatments of zirconia, like laser treatment, selective infiltration technique, hot etching solution, nano-structured alumina coating, and slurry-coated ceramic have been produced to advance and increase the surface roughened area to enable the mechanical interlocking of the ceramic and bonding resin (Noda et al, 2010) (Casucci et al, 2010).

1.9.1 Airborne-particle abrasion (APA) with alumina particles

The effectiveness of air abrasion with aluminum oxide particles (Al_2O_3) has been studied and is thoroughly correlated to the sandblasted ceramic surface and the air abrasion technique. Sandblasting has a significant role in advancing micromechanical retention by increasing surface roughness, wettability, surface energy, and surface area (Pereira et al, 2015) (Heikkienn, 2007).

Alumina is less ductile, and has greater grains and higher surface hardness, which makes air abrasion more effective (Lung and Matinlinna, 2012). According to abrasion with aluminum oxide particles, a wide range of particle sizes, pressure, distance from the ceramic surface, working time, and impact angle have been reviewed. Moon et al (2016)

claimed that the increase in surface roughness was proportional to the size of particles, duration of sandblasting, and angle of impact.

On yttrium-stabilized tetragonal zirconia (Y-TZP) material, the use of larger particle size (from 50 μm to 150 μm) leads to rougher surface but no significant alteration in bond strength (Tsuo et al, 2006). Evaluating a Y-TZP, Cavalcanti et al. (2009) revealed an increase in bond strength after air abrasion with 50 μm Al_2O_3 for 15 seconds at 2.5 bars.

It has been discovered that airborne-particle abrasion followed by the use of resin cement containing methacryloyloxydecyl dihydrogen phosphate (MDP) lead to the highest shear bond strength with zirconia restorations (Ozcan and Vallittu, 2003) (Blatz et al, 2007) (Wolfarrt et al, 2007).

A number of factors influence the fracture toughness of zirconia restorations. Albakry et al. (2004) claimed that sandblasting at close distance may reduce the mechanical properties by developing micro-cracks on the material surface. But other researchers propose that using resin cement types after airborne-particle abrasion can counteract cracks and apply a healing effect on the material surface (Burke et al, 2002) (Kelly and Denry, 2008).

Wang et al. (2007) revealed that the particle size used in the airborne-particle abrasion procedure governs the degree of impact damage. They discovered that sandblasting with 50 μm particles improved the strength of zirconia material, while 120 μm particles reduced the strength. The pressure placed during airborne-particle abrasion is critical as well. Heikkinen et al. (2007) stated that greater pressure in abrasion led to a rougher zirconia surface due to the higher kinetic energy of the abrasive particles. Finger

et al. (2020) claimed that the angulation of the sandblasting pen influenced the surface roughness of zirconia material, with the greatest surface roughness values attained with sandblastings perpendicular to the sample surface.

1.9.2 Hydrofluoric Acid (HF) Etching

Hydrofluoric acid, which is the inorganic acid hydrogen fluoride, has numerous industrial applications such as etching silica-based materials, pre-electroplating metal surface cleaning, and etching silicon wafers in electronic semiconductor materials (Hatzifotis et al, 2004) (Ozcan et al, 2012). In dental practice and laboratories, hydrofluoric acid concentrations ranging between 4% to 10% are frequently used. These concentrations are thought to be safe for dental applications (Alex, 2008). From a chemical standpoint, hydrofluoric acid works by softening glass via a reaction with silicon oxide, the primary component of glass. Dental porcelain comprises glassy and crystalline phases. Hence, hydrofluoric acid can dissolve the glassy phase, though leaving the crystalline phase intact, leading to the creation of surface roughness (Blatz, 2003) (Pisanai-Proenca, 2006).

1.10 Mechanical properties

Each dental material has its uses and limitations. A lot depends on its mechanical, physical, and optical characteristics. For a particular clinical scenario, a clinician would contemplate these properties in order to make a right choice.

Table 1: Summary of mechanical properties of materials used in this study

Materials	Mechanical properties				Composition
	Flexural Modulus hardness (GPa)	Fracture toughness (MPa·m ^{1/2})	Biaxial Flexural Strength (MPa)	Weight % of inorganic content	
Pacdent Rodin Sculpture 2	12.5	2.9	200	60%	Methacrylic Esters 25-49%, Photoinitiators 1-3%, Dimethacrylate based resin, inhibitor, fumed silica, and pigments
Sprintray Ceramic Crown	7	1.8	150	50%	Oligomers 20-60%, Monomers 20- 50%, Photoinitiators 0.1-10%, Additives 10-60%
Rodin Titan	4	3.7	140	50%	Methacrylic esters (25-49%), Photoinitiators 1-3%

Layzir Zirconia	13.0 ± 0.1	4.1 ± 0.4	> 900	NA	Zirconium dioxide ZrO ₂ (79-96%), Hafnium dioxide HfO ₂ <5%, Yttrium oxide Y ₂ O ₃ <10%, other oxides <16%
------------------------	----------------	---------------	-------	----	---

1.11 Purpose of the study

The purpose of this in-vitro study aimed to investigate bonding efficiency, measure bonding of multi and single step cements to printed resins and Layzir zirconia. Also, to evaluate the effect of different material combinations on shear bond strength, and to evaluate the effect of thermocycling on shear bond strength of different materials combinations.

1.12 Objectives

- Determine the shear bond strength of multi and single step cements to printed resins, and Layzir Zirconia.

- Evaluate the effect of different material combinations of shear bond strength.
- Evaluate the effect of thermocycling on shear bond strength of different materials combinations.
- Evaluate the mode of failure on shear bond strength.

1.13 Null hypothesis

- No significant differences exist in the effects of various cement types on their shear bond strength to zirconia and resins.
- The use of different material/cement combinations has no effect on shear bond strength of the final restoration.
- Thermocycling has no effect on shear bond strength of different materials combinations.

CHAPTER 2. MATERIALS & METHODS

2.1 Materials

The materials used in this study were as followed (Figure 1):

Print Resins:

A) PacDent Rodin Sculpture 2.0 (REF: 23871. Shade B1, Lot #310080, Exp 11/2024)

B) SprintRay Ceramic Crown. (REF: SR1#0202886, Shade A2, Lot #S23B22CA21, Exp 07/22/2024)

C) Rodin Titan. (REF: 23985, Shade B1, Lot #311002, Exp 11/2024)

Ceramics:

D) Layzir Zirconia (REF: CM0056S, shade 1M1, Lot #DBU222L27F, Exp 12/2032)



Figure 1. Materials used in the study. A) Pacdent Sculpture 2.0 B) SprintRay Ceramic Crown, C) Rodin Titan, and D) Layzir Zirconia

Cements and bonds:

Self-adhesive resin cement includes:

- Panavia SA Cement universal Auto mix (P-SA) (Kuraray) (Lot no. 850196 /shade; universal A2) (Figure 2).



Figure 2. Panavia SA cement used in the study

Adhesive resin cement includes:

- Panavia V5 Cement Auto mix (P-V5) (Kuraray) (Lot no. 000092 /shade; universal A2) (Figure 3).



Figure 3. Panavia V5 cement used in the study

- Resicem EX cement ResiCem is a radiopaque, dual-cure, resin-based, adhesive cementation system (Shofu Dental Corporation) (Lot no. 052312/ shade: Ivory) (Figure 4).



Figure 4. Resicem Ex cement used in the study

- HC Primer is a single component primer developed to treat the bonding surface of CAD/CAM ceramic filler contained composite (Shofu Dental Corporation) (Lot #112310) (Figure 5).



Figure 5. HC primer used in the study

- AZ primer: priming agent designed to treat the surfaces of alumina-based or zirconia-based restorations to enhance bond to resin materials (Shofu Dental Corporation) (Lot #052347) (Figure 6).



Figure 6. A. AZ primer used in the study B. Rodin bond used in the study

- Rodin Bond; Rodin® Bond, a light-cured dental adhesive (Figure 6B)
- SensiGuard™: desensitizer and primer promote bonding, seals dentin tubules to prevent sensitivity (PacDent) (Figure 6B).

- 5% HF gel: VITA Ceramics Etch 6ml (VITA Zahnfabrik) (Lot no:91220).
- Clearfil ceramic primer plus (Kuraray, Osaka, Japan).
- Aluminum oxide particles, 50-125 μm (Renfert GmbH, Hilzingen, Germany).

Table 2. Characteristics of cements used in the study

Cement	Composition	Bonding	Filler (wt%)	Curing mode	Manufacturer	Bond strength values
P-SA	<p>Paste A: 10- (MDP)/ (Bis-GMA)/ (TEGDMA)/ Hydrophobic aromatic dimethacrylate. (HEMA)/Silanated barium glass filler/Silanated colloidal silica/dl-Camphorquinone/ Peroxide/Catalysts/ Pigments.</p> <p>Paste B: Hydrophobic aromatic dimethacrylate/ Silane coupling agent/ Silanated barium glass filler/Aluminum oxide filler/Surface treated sodium fluoride (Less than 1%)/ dl-Camphorquinone/ Accelerators/Pigments.</p>	Self-adhesive Resin cement	<p>Inorganic filler: 40 vol%</p> <p>Particle size of inorganic fillers: 0.02 μm to 20 μm</p>	Dual cure	Kuraray Medical, Okayama, Japan.	$\approx 25\text{-}27$ MPa

P-V5	Silanated barium glass filler/Hydrophobic aromatic dimethacrylate/Bis-GMA/Silanated fluoroalminosilicate glass filler/Hydrophilic aliphatic dimethacrylate/Silanated titanium dioxide (0-5 % by mass)/TEGDMA/ Surface treated aluminum oxide filler/Colloidal silica/dl-Camphorquinone/Initiators/Accelerators/ Pigments.	Adhesive resin cement	Inorganic filler: 38 vol% Particle size of inorganic fillers: 0.01 μm to 12 μm	Dual cure	Kuraray Medical, Okayama, Japan.	\approx 27-30 MPa
Resicem EX	Paste A: UDMA, TEGDMA, S-PRG filler, bis-GMA, silicate glass, initiators, others. Paste B: UDMA, TEGDMA, Carboxylic acid monomer, 4-AET, 2-HEMA S-PRG filler, bis-GMA, silicate glass, initiators, others	Resin based adhesive cement	65 wt.%, 45 vol.%	Dual cure	Shofu, Kyoto, Japan	\approx 20-22 MPa

Table 3. Characteristics of Adhesives/primers used in the study

Adhesive/Primer	Manufacturer	Composition
Clearfil ceramic primer plus	Kuraray Medical, Okayama, Japan.	Ethanol, methacryloyloxypropyltrimethoxysilane, 10- Methacryloyloxydecyl dihydrogen phosphate

HC Primer	Shofu Dental Corporation	Urethane dimethacrylate (UDMA), Methyl methacrylate (MMA), polymerization initiator, acetone
AZ Primer	Shofu Dental Corporation	6-MHPA(6-methacryloxyhexylphosphonoacetate), acetone, others
Rodin Bond	PacDent	Ethanol, 2-Hydroxyethyl methacrylate, 2-hydroxy-1, 3-Propanediyl bismethacrylate, Alkali fluorosilicates (Na)

Stainless steel used in the study:

- Universal Stainless-Steel rods (Shofu Dental Corporation) (Figure 7).
- The stainless-steel rod dimension measurement is 10 mm for the height, 4 mm for the diameter.



Figure 7. stainless-steel rods used in the study

2.2 Equipment:

- Asiga 3D Printer (Figure 8).

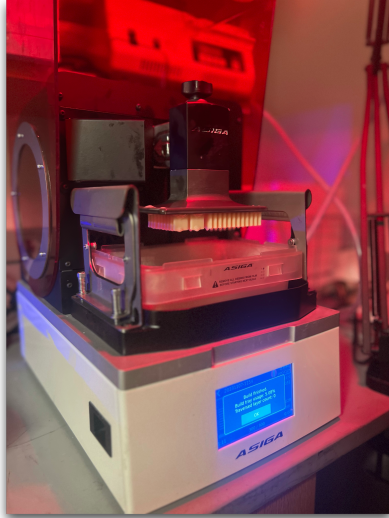


Figure 8. Left Aiga 3D printer used in the study. Right Otoflash G171

- Instron 5566A Universal Testing Machine (Instron, Norwood, MA, USA) (Figure 9).



Figure 9. Instron 5566A Universal Testing Machine

- Section machine (BUEHLER Isomet- 5000 precision saw) with a diamond blade speed of 2000 rpm, blade thickness of 0.5mm, under running water (Figure 10).



Figure 10. BUEHLER Isomet-5000 precision saw

- Thermocycling test apparatus (Sabri Dental Enterprises, USA) (Figure 11).



Figure 11. Thermocycling test apparatus

- Sandblaster: Renfert Basic Quattro IS (Renfert, Hilzingen, Germany) (Figure 12).



Figure 12. Sandblaster: Renfert Basic Quattro

- **Fisher Scientific Oven** (Thermo scientific, OH, USA) (Figure 13).



Figure 13. Fisher Scientific Oven (Thermo scientific, OH, USA)

- Sintering oven: Hot spot 110 Lab furnace (Zircar zirconia, Inc, NY, USA) (Figure 14).



Figure 14. Sintering oven: Hot spot 110 lab furnace

- Incubator (Precision-Economy Incubator, Precision Scientific, Winchester, VA, USA).
- Demi Plus L.E.D Curing Light (Kerr Corporation, California, USA).
- Grinder-polisher machine. Buehler, EcoMet[®] 250.

2.3 Methods:

2.3.1 Material preparation

3D printing of resins was done using the Asiga 3D printer (Figure 8), a flat plate of the crown resin materials 2 mm thick and 15 mm height and width were designed on Asiga Composer software (version 1.3.3), the material to be printed was chosen (print resolution 62 μm).

To start the build, the vat/tray was inserted, and approximately 10 mm thickness of resin was poured into the vat.

PacDent Rodin Sculpture, SprintRay Ceramic Crown and Rodin Titan resin specimens were printed (Figure 1). On completion of printing, the print objects were detached from the build platform using the spatula supplied.

To remove excess resin, wet paper towel or cloth soaked with 99% IPA (optimal concentration) was used on specimens to remove excess uncured resin.

Post-curing was performed in a validated UV LED light-cure heat-cure box using NK-Optik Otoflash G171 4500 flashes with inert gas (99.94% pure nitrogen) (Figure 8).

The completely cured objects were stored in a room temperature and protected from sources of bright light.

Layzir Zirconia specimens were prepared by sectioning the zirconia disc using the Isomet 5000 sectioning machine (Figure 15), into blocks, then blocks were sectioned into plate-shape specimens (2mm \times 14mm \times 14mm). Each specimen was polished on the edges to remove any sharp ends or irregularities after sectioning, all pre-sintered bars were polished

with a 240/P280 grit sandpaper to remove any sharp edges. All specimens were then sintered in a Zircar furnace (Figure 14) to produce fully sintered (FS) zirconia with an approximate volumetric shrinkage of 18.76%. A heating rate of 10°C/min from room temperature to 1450°C with a holding time of 2h was used. The total amount of time for the firing process was 6 h 30 m.

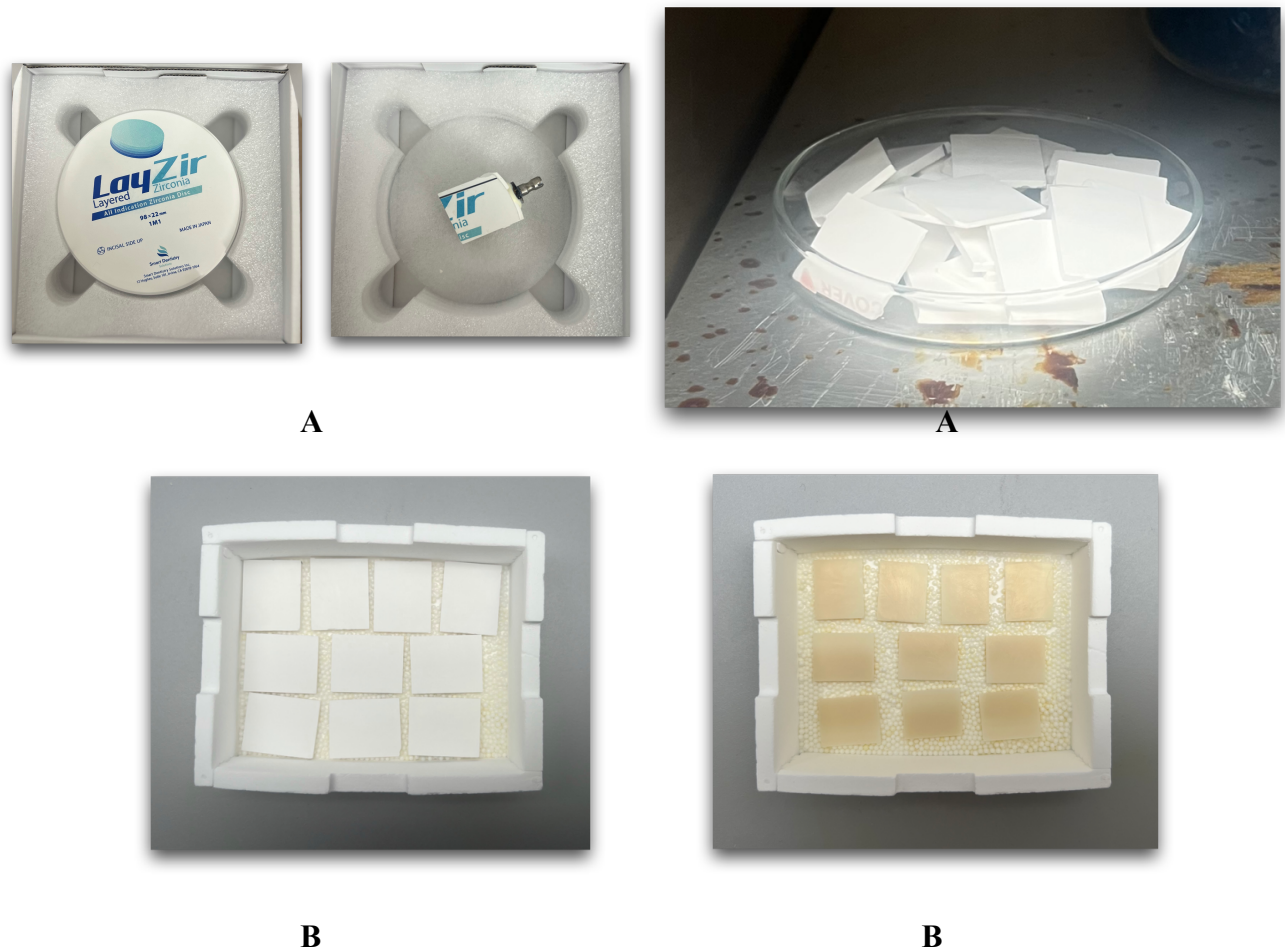


Figure 15. Layzir Zirconia specimen preparation. A) Disc sectioned into blocks, then blocks into plates. B) Prepared specimens were sintered in Zircar furnace.

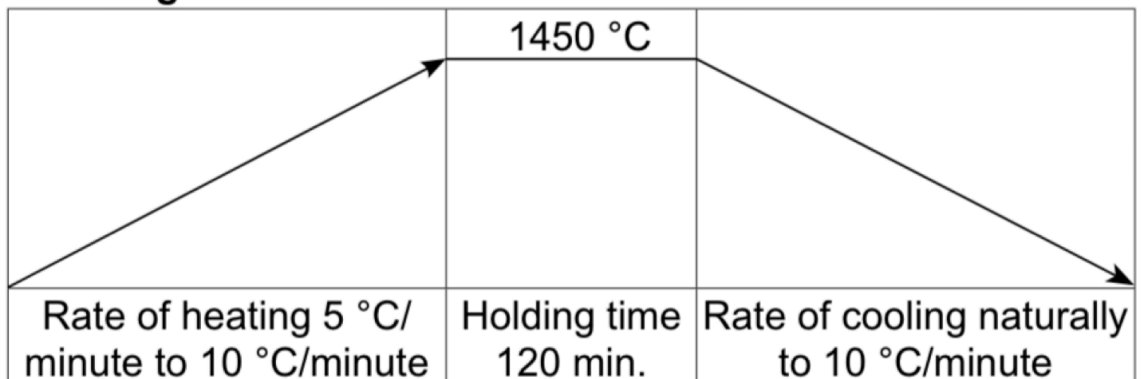


Figure 16. Recommended sinter program

1450 °C for 2.25 hrs. (Heating rate)

1450 °C for 2 hrs. (Holding time)

200 °C for 2.05 hrs. (Rate of cooling naturally)

2.3.2 Surface preparation

- Airborne-particle abrasion of fully sintered zirconia:

The fully sintered zirconia was sandblasted with a 50 µm aluminum oxide particle size with an airborne-particle abrasion machine (Renfert Basic Quattro IS, Renfert, Hilzingen, Germany) (Figure 12) using 2.5 bar of pressure at 2-5 mm for 10 seconds. Then, the zirconia was cleaned in an ultrasonic cleaning bath with de-ionized water for three minutes and dried in an oven (Fisher Scientific oven) for 30 minutes at 85-100°C.

All materials were surface treated based on material recommendations prior to bonding.

All stainless-steel rods were sandblasted with 125 µm Al₂O₃ at a pressure of 2.5 bar.

Zirconia, and Sprint Ray Ceramic crowns were sandblasted with 50 μm Al_2O_3 at a pressure of 2.5 bar for 10 seconds as described in Table 4.

Paccdent Rodin Sculpture 2, Sprintray Ceramic Crown and Titan were conditioned using 5 % hydrofluoric acid etch gel (VITA Zahnfabrik) for 60 seconds then washed with distilled water for 20 seconds and dried with oil-free compressed air (Table 4).

Table 4. Surface treatment for all materials prior to bonding

Framework materials (plates)	Surface Treatment before bonding
Paccdent Sculpture 2	5 % hydrofluoric acid gel (Vita ceramics) for 60 seconds
Sprintray Ceramic Crown	Sandblast with 50 μm Al_2O_3 at a pressure of 2.5 bar (Renfert GmbH, Hilzingen, Germany), 5 % hydrofluoric acid gel for 60 seconds (Vita ceramics)
Titan	5 % hydrofluoric acid gel for 60 seconds
Layzir Zirconia	Sandblast with 50 μm Al_2O_3 at a pressure of 2.5 bar with 10 mm nozzle distance
Materials (rods)	Surface Treatment before bonding
Stainless steel Rods	Sandblast with 125 μm Al_2O_3 at a pressure of 2.5 bar With 10 mm nozzle distance

2.3.3 Cementing process

Cementing process using Panavia SA, Panavia V5, Resicem EX:

The surfaces of both the stainless-steel rod and frameworks were thoroughly dried with compressed air (30 psi).

- Panavia SA Cement Universal Auto mix cement was applied on the resin specimen and Layzir Zirconia surface. Clearfil Ceramic Primer plus was only used on specimens bonded with Panavia V5. Rodin Bond was only used on samples cemented with Panavia V5, and HC primer for resin bonding and AZ primer for Zirconia were only used for specimens bonded with Resicem EX.
- In the last stage of specimen preparation, the framework plate was placed on a flat surface, then the adhesive resin cement was injected to fill the bonding area between the framework and the rod. The stainless-steel rods were gently seated on the middle of the resin plate, allowing the cement to flow from all margins to leave a slightly excess amount. The rod/framework complex was placed under a 1393 g (1.4 kg/13.66N) weight load for 10 minutes in a cylindrical loading apparatus (Figure 17). While the specimen was under load, light curing for 3-4 seconds was performed using a Demi Plus L.E.D Curing Light (Kerr Corporation, California, USA) intensity of 1,100 mW/cm² to a peak of 1,330, then excess cement was removed around the rod border with a plastic instrument. Then a full cure for 20 seconds was applied using a Demi Plus L.E.D Curing Light (Kerr Corporation, California, USA) on High mode. All specimens were placed in a 37-degree

incubator (Precision Economy Incubator, Precision Scientific, 5EM model, USA) for 24 hours in a moist, sealed container before shear bond testing was conducted.

- 384 specimens are divided into 16 groups according to material combinations, static or thermal aging process.



Figure 17. Top: Before and after bonding framework plate and rod. Bottom: All framework plates and veneer rods were bonded; excess cement was removed and bonded. The specimens were kept under a static load of 1393 g (1.4 kg/13.66N) for 10 minutes in a cylindrical loading apparatus.

2.4 Thermocycling

All 8 groups after bonding were subjected to a thermal aging process (Figure 11); all specimens were packed in a plastic, porous mesh bag and then underwent 5000 thermocycles (between 5 and 55°C) with a 30-second dwell time in each water bath by using a thermocycling test apparatus (Sabri Dental Enterprises, USA) before the shear bond test.

2.5 Shear Bond testing

In this study, 384 specimens were divided into sixteen groups (n=16) according to framework/cement/rod material combinations, static or thermal aging process (Table 5). Half of the specimens (192 samples) were allocated into 16 control groups where no thermal aging was done, while the other six groups (192 samples) were assigned to undergo thermal cycling process before shear bond testing.

Compressed air was used to gently dry objects and placed in a dark drawer away from direct light, in room temperature for 30 minutes to completely dry. A shear bond test was performed on all static and thermocycled specimens' groups by using the universal testing machine (Instron 5566A) to perform the test at a crosshead speed of 0.5 mm/min with a 1 kN load cell. Specimens were placed in the shear bond testing apparatus using a flat shear/knife edge blade to shear the pins (Figure 18). The knife edge/sharp blade had a perpendicular contact at the interface between the rod and underlying framework plate. A load was applied at the adhesive interface between the framework plate/rod during the testing. The bond strength was calculated in MPa by dividing the load by the cross-

sectional area of the bonded specimens. The maximum shear load was recorded at debonding.

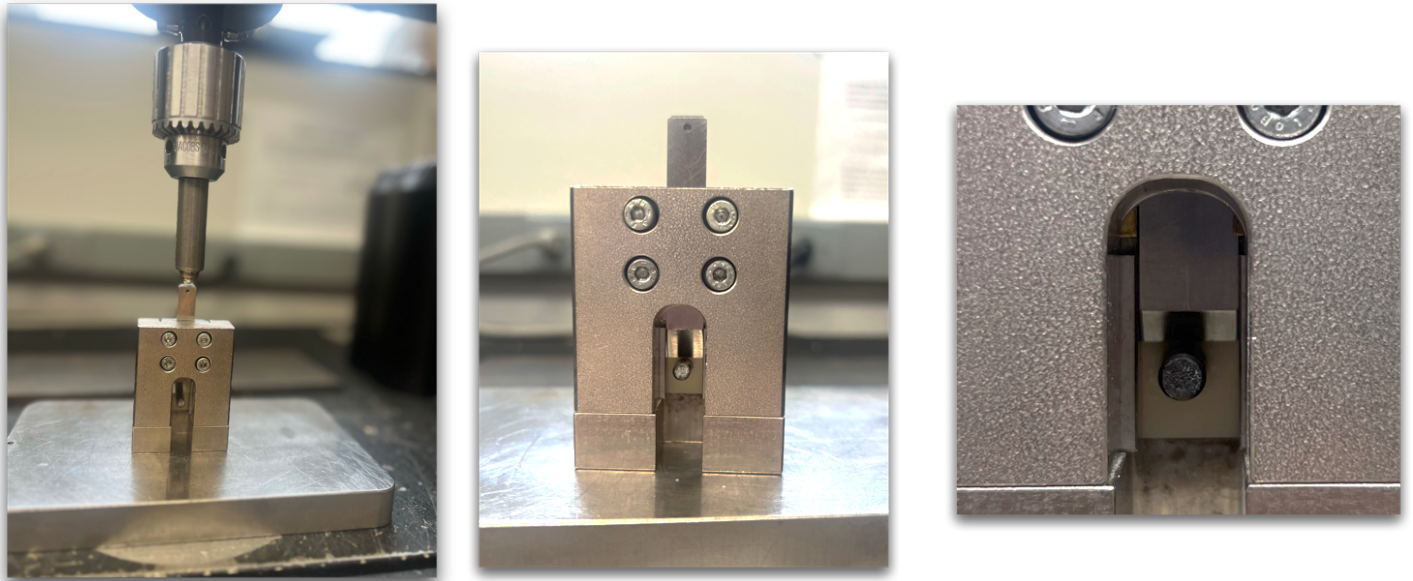


Figure 18. Specimens were placed in the shear bond test fixture. A flat/knife edge blade was used to shear the rods.

2.6 Failure mode analysis using digital microscope

The failure mode was examined using Keyence Digital Microscope (Figure 19).



Figure 19. Keyence Digital Microscope

Table 5. Material-cement-bond combination

Group	Plate	Cement	Bond	Surface treatment	Rods	N (Control)	N (T/C)
1	Pacdent Sculpture 2	Panavia V5	Rodin Bond	Sandblasting Rod Etching plate	Stainless Steel Rod	12	12
2	Sprintray Ceramic Crown	Panavia V5	Rodin Bond	Sandblasting both Etching plate	Stainless Steel Rod	12	12
3	Titan	Panavia V5	Rodin Bond	Sandblasting Rod Etching plate	Stainless Steel Rod	12	12
4	Layzir Zirconia	Panavia V5	Rodin Bond	Sandblasting both	Stainless Steel Rod	12	12
5	Pacdent Sculpture 2	Panavia V5	Clearfil Primer	Sandblasting Rod Etching plate	Stainless Steel Rod	12	12
6	Sprintray Ceramic Crown	Panavia V5	Clearfil Primer	Sandblasting both Etching plate	Stainless Steel Rod	12	12
7	Titan	Panavia V5	Clearfil Primer	Sandblasting Rod Etching plate	Stainless Steel Rod	12	12
8	Layzir Zirconia	Panavia V5	Clearfil Primer	Sandblasting both	Stainless Steel Rod	12	12
9	Pacdent Sculpture 2	Panavia SA	■	Sandblasting Rod Etching plate	Stainless Steel Rod	12	12
10	Sprintray Ceramic Crown	Panavia SA	■	Sandblasting both Etching plate	Stainless Steel Rod	12	12

11	Titan	Panavia SA	■	Sandblasting Rod Etching plate	Stainless Steel Rod	12	12
12	Layzir Zirconia	Panavia SA	■	Sandblasting both	Stainless Steel Rod	12	12
13	Pacdent Sculpture 2	Resicem EX	HC Primer	Sandblasting Rod Etching plate	Stainless Steel Rod	12	12
14	Sprinray Ceramic Crown	Resicem EX	HC primer	Sandblasting both Etching plate	Stainless Steel Rod	12	12
15	Titan	Resicem EX	HC Primer	Sandblasting Rod Etching plate	Stainless Steel Rod	12	12
16	Layzir Zirconia	Resicem EX	AZ Primer	Sandblasting both	Stainless Steel Rod	12	12

2.7 Statistical Analysis:

Descriptive statistics such as shear bond strength, maximum load and mode of failures were indicated as mean and standard deviation (SD). The level of significance was set at p-value < 0.05 . A one-way ANOVA test was used to compare the means among the different groups. Tukey's test was also utilized to determine the significant differences among the groups tested. All statistical analyses were performed using JMP Pro (Version 17.2.0).

CHAPTER 3. RESULTS

3.1 Shear bond test results

A shear bond test in this study was performed to evaluate the bond strength of different cements to zirconia and 3D printed materials and evaluate the effect of thermal aging on the shear bond strength.

The mean shear bond (MPa), standard deviations (SD), and coefficient of variance (CV) were calculated for the control and treated groups (Table 6). Twelve (12) specimens per group were prepared and processed for each group. Box plots were used to identify outliers, which were excluded in the final statistical analysis; also, premature failure specimens were not included, which were found mostly in the thermocycling treatment groups. Hence, N values used for final statistical analysis differ in each group.

Table 6. SBS and mode of failure of different cement and material combinations

			<u>Shear Bond Strength (MPa)</u>				<u>Mode of Failure</u>			
Layzir Zirconia	Cement + Bond	Post Treatment	N	Mean	Std Dev	CV	Adhesive	Adhesive/ Cohesive	Cohesive	Premature failure
	Panavia SA no bond	Control	10	22.46	7.18	31.97	10	0	0	0
		Thermocycled	10	21.70	11.36	52.37	10	0	0	0
	Panavia V5 + Clearfil	Control	12	24.52	8.38	34.21	10	2	0	0
		Thermocycled	11	11.71	6.25	53.37	11	0	0	0
	Panavia V5 + Rodin Bond	Control	13	15.06	5.14	34.12	13	0	0	0
		Thermocycled	6	8.76	6.75	77.15	6	0	0	4
	Resicem + Primer	Control	12	20.01	4.64	23.19	12	0	0	0
		Thermocycled	11	6.13	1.88	30.73	11	0	0	0
PacDent Sculpture 2	Cement + Bond	Post Treatment	N	Mean	Std Dev	CV	Adhesive	Adhesive/ Cohesive	Cohesive	Premature failure
	Panavia SA no bond	Control	8	25.51	5.91	23.17	8	0	0	0
		Thermocycled	11	19.53	5.30	27.13	3	0	8	0
	Panavia V5 + Clearfil	Control	15	13.62	5.83	42.84	14	1	0	0
		Thermocycled	8	11.06	4.92	44.48	8	0	0	4
	Panavia V5 + Rodin Bond	Control	10	23.02	3.14	13.64	0	0	10	0
		Thermocycled	8	10.45	5.21	49.90	8	0	0	4
	Resicem + Primer	Control	12	31.99	9.35	29.24	2	0	10	0
		Thermocycled	11	16.80	11.46	68.19	8	0	3	0
SprintRay	Cement + Bond	Post Treatment	N	Mean	Std Dev	CV	Adhesive	Adhesive/ Cohesive	Cohesive	Premature failure
		Control	11	32.07	6.52	20.35	9	0	2	0

	Panavia SA no bond	Thermocycled	11	23.45	4.41	18.82	0	2	9	1
	Panavia V5 + Clearfil	Control	9	17.26	1.98	11.48	9	0	0	0
		Thermocycled	6	20.91	1.70	8.15	0	0	6	0
	Panavia V5 + Rodin Bond	Control	12	19.13	6.27	32.81	10	0	2	0
		Thermocycled	12	12.31	5.92	48.05	9	0	3	0
	Resicem + Primer	Control	10	23.41	6.58	28.11	2	1	7	0
		Thermocycled	11	16.33	5.09	31.18	9	0	2	0
Titan	Cement + Bond	Post Treatment	N	Mean	Std Dev	CV	Adhesive	Adhesive/ Cohesive	Cohesive	Premature failure
	Panavia SA no bond	Control	12	29.50	6.75	22.91	12	0	0	0
		Thermocycled	11	16.03	4.75	29.62	7	0	4	0
	Panavia V5 + Clearfil	Control	10	30.91	7.94	25.71	10	0	0	0
		Thermocycled	12	12.11	7.01	57.88	12	0	0	0
	Panavia V5 + Rodin Bond	Control	11	21.24	6.20	29.18	10	0	1	0
		Thermocycled	7	7.43	5.59	75.26	7	0	0	5
	Resicem + Primer	Control	12	24.73	5.35	21.63	5	0	7	0
		Thermocycled	10	17.70	7.07	39.93	7	0	3	0

Table 7. Effect summary of material, cement-bond, and post-treatment on SBS

Source	LogWorth	P Value	
Post treatment	27.64	0.00000	
Cement+Bond	14.65	0.00000	
Material*cement+Bond	7.28	0.00000	
Material	3.36	0.00043	^
Material*Posttreatment	2.44	0.00359	
Posttreatment*Cement+Bond	0.45	0.35122	

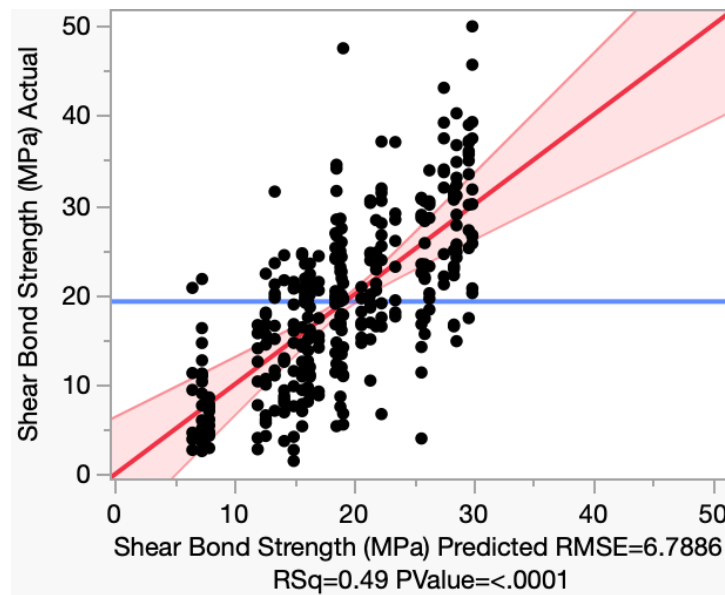


Figure 20. Actual whole model of SBS of all groups by predicted plot ($R^2=0.49$, P-value<0.0001)

The analysis from a least square mean linear regression model showed R square= 0.49, which indicated that a 49% variance could be predicted by the established model, and p-value <0.0001, which indicated significant effects (Figure 20). The tested factors had a significant effect on the shear bond strength. The dominant effects on SBS were thermocycling aging (P-value <.0001), cement-bond combinations (p-value <.0001), and material × cement-bond interaction (P-value <.0001) (Table 7).

The logworth column (Table 7) (Figure 20) shows the significant effect each factor has on the shear bond strength. It can be shown that post treatment (thermocycling) does have a significant effect on SBS, as well as interacting with material type (P-value = 0.0004) using different cement-bond and material combinations. Whereas on the other hand, post treatment × cement and bond interaction does not have a significant effect on SBS values (P-value = 0.35). In this study, pooled data has been presented below, in order to provide a more comprehensive precise data set, as outliers and unevenly distributed data skew the result.

3.1.1 SBS affected by different material.

Least square mean regression results show significantly higher ($P=0.0004$) SBS among the resin groups compared to Layzir zirconia group showed in Figure 21 and Table 8.

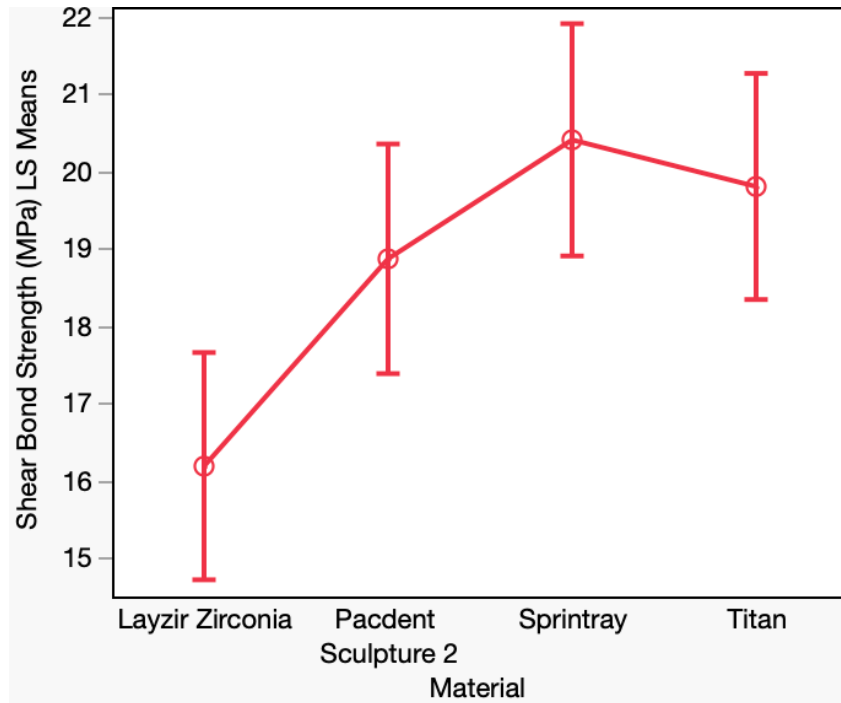


Figure 21. SBS least square mean plot affected by different material combinations.

Table 8. Connecting letters report for comparing different group materials on SBS values among all groups using Tukey-Kramer HSD

Level			Least Sq Mean
SprintRay	A		20.40
Titan	A		19.80
PacDent Sculpture 2	A	B	18.86

Layzir Zirconia		B	16.18
-----------------	--	---	-------

3.1.2 SBS affected by cement-bond

Figure 22 and Table 9 show that cement-bond has a statistically significant effect on SBS (P-value <0.0001). Panavia SA cement is significantly higher (P-value<0.0001) than Panavia V5 bonded with Clearfil (P-value<0.0001) and Rodin bond (P-value<0.0001), and Resicem cements (P-value=0.0003).

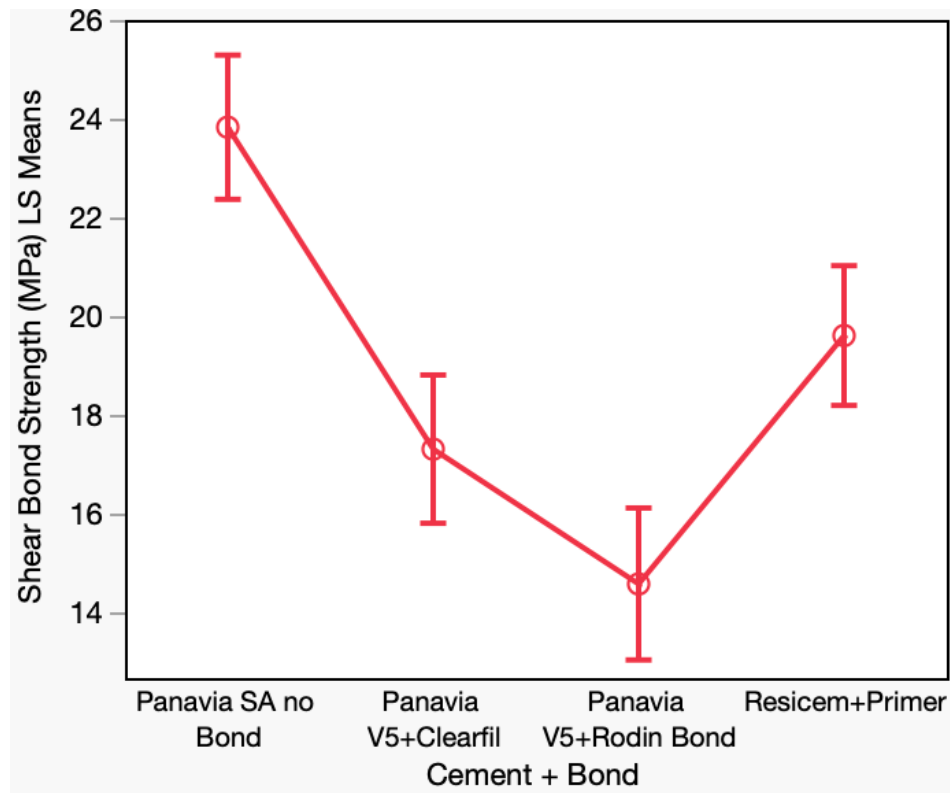


Figure 22. SBS least square mean plot affected by cement-bond combination

Table 9. Connecting letters report for comparing different cements on SBS values among all groups using Tukey-Kramer HSD

Level				Least Sq Mean
Panavia SA No bond	A			23.82
Resicem + Primer		B		19.59
Panavia V5 + Clearfil		B	C	17.28
Panavia V5 + Rodin Bond			C	14.55

3.1.3 SBS affected by post-treatment.

It is shown in Figure 23 and Table 10 post-treatment (thermocycling) has a statistically significant effect (P-value<0.0001) on SBS. The Control groups are significantly higher (P-value<0.0001) than the thermocycled groups.

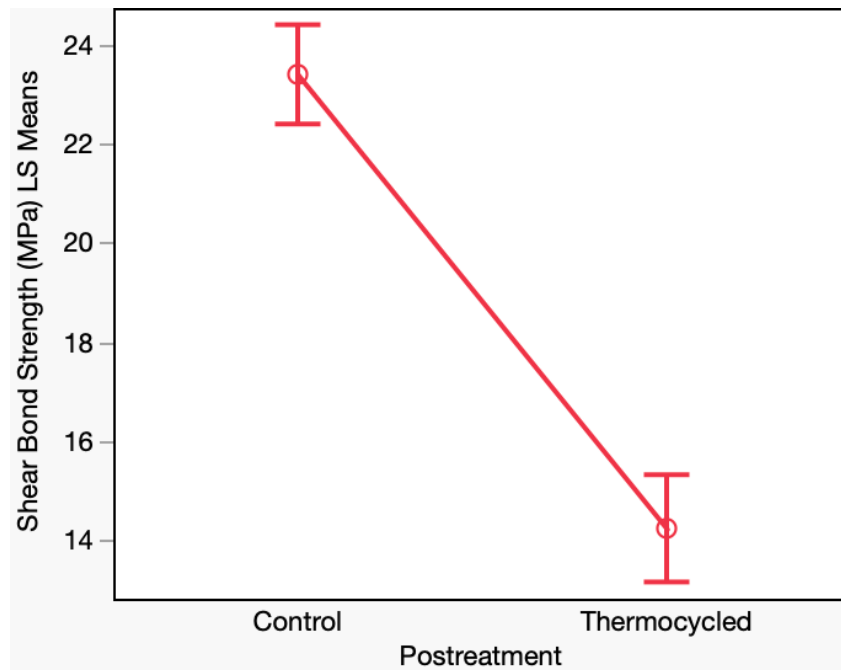


Figure 23. SBS least square mean plot between control and post-treatment groups

Table 10. Summary of mean of control and thermocycled groups

Level	Sq Mean	Std error	Mean
Control	23.41	0.51	24.14
Thermocycled	14.21	0.55	14.74

3.1.4 SBS affected by material and cement-bond system interaction.

It is shown in Figure 24 and Table 11 that material and cement-bond interaction has a significant effect ($P\text{-value} < 0.0001$) on SBS. SprintRay bonded with Panavia SA materials produced the highest shear bond strength least mean square values (27.76 MPa) compared to other groups, followed by PacDent Sculpture 2 bonded with HC primer and Resicem

(24.49 MPa), Titan and PacDent Sculpture 2 bonded with Panavia SA (22.81MPa, 22.63 MPa).

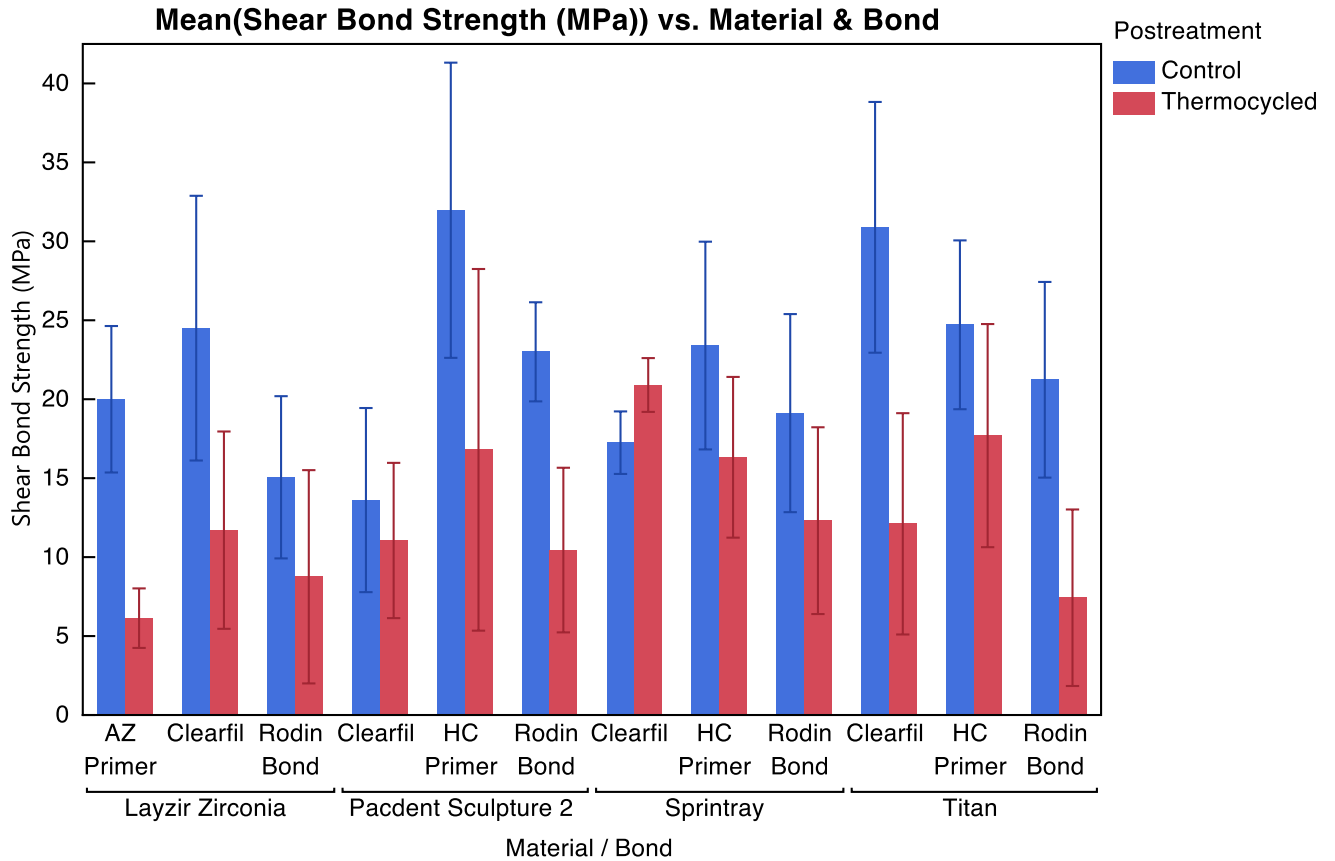


Figure 24. Bar chart of mean shear bond strength of the tested groups

Table 11. Connecting letters report for comparing different materials and cement-bond on SBS values using Tukey-Kramer HSD

Level							Least Mean	Sq
Sprintray, Panavia SA no bond	A						27.76	

Paccdent Sculpture 2, Resicem+Primer	A	B						24.49
Titan, Panavia SA no bond	A	B	C					22.81
Paccdent Sculpture 2, Panavia SA no bond	A	B	C	D				22.63
Layzir Zirconia, Panavia SA no bond	A	B	C	D				22.08
Titan, Panavia V5+Clearfil	A	B	C	D	E			21.23
Titan, Resicem+Primer	A	B	C	D	E			20.85
Sprintray, Resicem+Primer		B	C	D	E	F		19.87
Sprintray, Panavia V5+Clearfil		B	C	D	E	F	G	18.25
Layzir Zirconia, Panavia V5+Clearfil		B	C	D	E	F	G	18.22
Paccdent Sculpture 2, Panavia V5+Rodin Bond			C	D	E	F	G	16.88
Sprintray, Panavia V5+Rodin Bond				D	E	F	G	15.72
Titan, Panavia V5+Rodin Bond					E	F	G	14.30
Layzir Zirconia, Resicem+Primer						F	G	13.14
Paccdent Sculpture 2, Panavia V5+Clearfil							G	11.45
Layzir Zirconia, Panavia V5+Rodin Bond							G	11.29

3.1.5 SBS affected by material and post-treatment interaction.

It is shown in Figure 25 and Table 12 that there is a statistically significant interactive effect between materials and post-treatment groups ($P = 0.0036$). The control groups are significantly higher than the thermocycled groups.

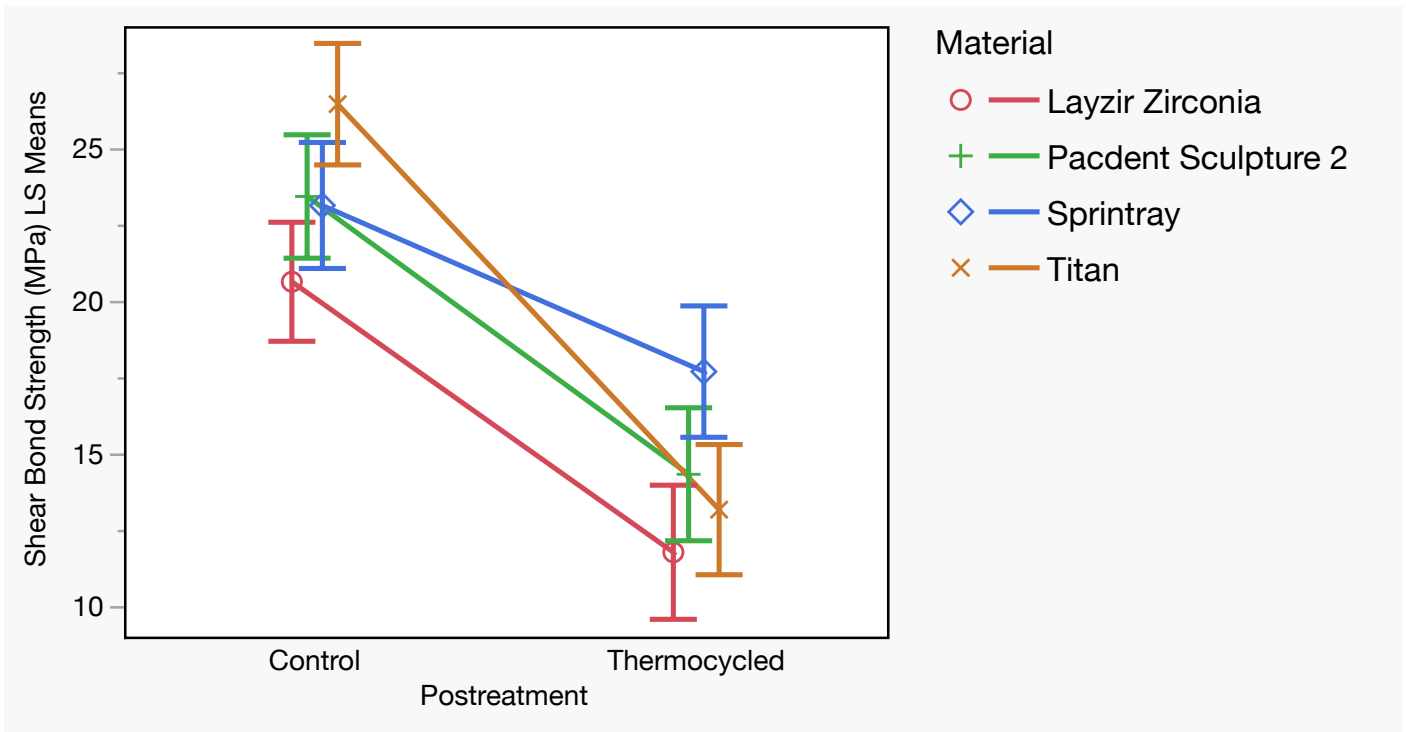


Figure 25. SBS least square mean plot between control and post-treatment groups

Table 12. Connecting letters report for comparing different materials on SBS values among all groups (control and thermocycled) using Tukey-Kramer HSD

Level					Least Sq Mean
Titan, Control	A				26.45
Pacdent Sculpture2, Control	A	B			23.42
Sprintray, Control	A	B			23.13
Layzir Zirconia, Control		B	C		20.62
Sprintray, Thermocycled			C	D	17.67

Pacdent Sculpture 2, Thermocycled					D	E	14.30
Titan, Thermocycled					D	E	13.14
Layzir Zirconia, Thermocycled						E	11.74

3.1.6 SBS affected by cement-bond and post-treatment interaction

Figure 26 and Table 13 show that there is no statistically significant interactive effect between different cements and bonding agents and post-treatment (P=0.35).

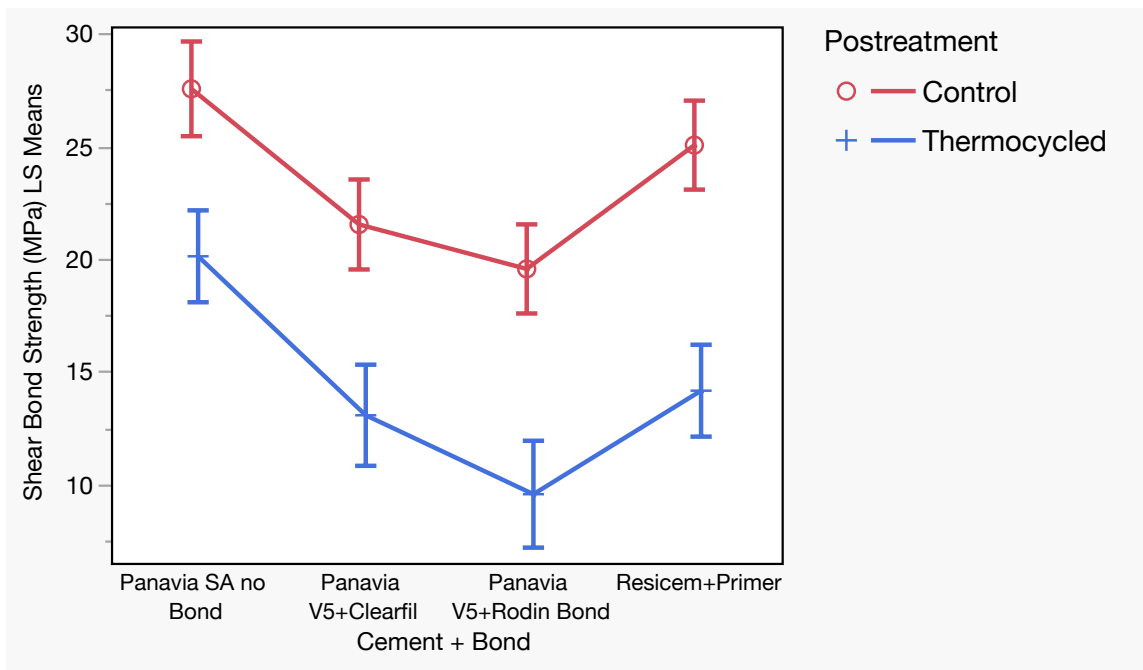


Figure 26. SBS least square mean plot affected by cement-bond combination in control and thermocycled group combinations

Table 13. Connecting letters report for comparing different cements on SBS values among all groups (control and thermocycled) using Tukey-Kramer HSD

Level					Least Sq Mean
Control, Panavia SA no bond	A				27.53
Control, Resicem+Primer	A	B			25.04
Control, Panavia V5+Clearfil		B	C		21.52
Thermocycled, Panavia SA no bond			C		20.10
Control, Panavia V5+Rodin Bond			C		19.54
Thermocycled, Resicem+Primer				D	14.14
Thermocycled, Panavia V5+Clearfil				D	13.05
Thermocycled, Panavia V5+Rodin Bond				D	9.55

3.2 Mode of failure

For SBS specimens, 384 specimens were analyzed after testing to evaluate the mode of failure of each specimen. The mode of failure was divided into 3 categories: adhesive, cohesive, and adhesive-cohesive (mixed). All specimens were observed using an optical microscope to observe the mode of failure among SBS groups. Where adhesive failure represents failure at interface of adhesive and substrate, while cohesive failure represents failure within the substrate (framework/rod or within the adhesive), and adhesive-cohesive (mixed) failure represents combination of adhesive and cohesive failures (Figure 27).



Figure 27. Mode of failures for SBS (Source: Instron, ASTM D1002 Lap Shear

Testing of Adhesively Bonded Materials)

Table 14. Descriptive of failure mode after SBS test in different cement-bonding agents

SBS groups	Failure Type						Total	
	Cohesive		adh-cohesive		Adhesive		N	%
	N	%	N	%	N	%		
Panavia SA no bond	23	27.06%	2	2.23%	59	69.41%	85	24.08%
Panavia V5+Clearfil	6	6.9%	3	3.45%	74	85.06%	87	24.65%
Panavia V5+Rodin Bond	16	17.39%	0	0.0%	63	68.48%	92	26.06%
Resicem+Primer	32	35.96%	1	1.12%	56	62.92%	89	25.21%
Total	77	21.81%	6	1.7%	252	71.39%	353	100.0%
Chi-square	χ^2	47.63						
	P-value	<0.001*						

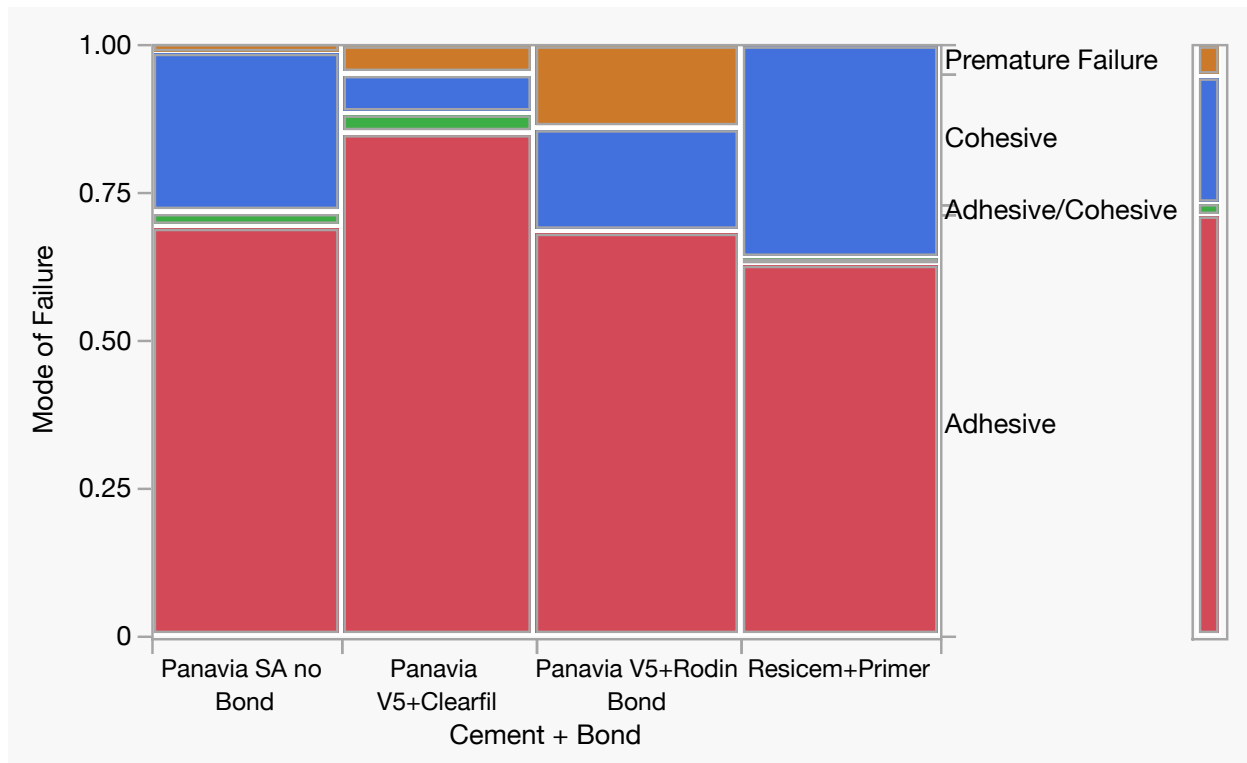


Figure 28. Mosaic plot of failure mode affected by cement-bond combination

Table 14 and Figure 28 show a significant difference regarding the failure mode, and cement-bonding agents used ($P\text{-value} < 0.0001$). 69.41% of Panavia SA specimens showed adhesive failures, 85.06% adhesive failures for Panavia V5 and Clearfil, 68.84% adhesive failures for Panavia and Rodin bond, and 62.92% for Resicem cement. Resicem cement showed the highest cohesive mode of failure 35.95%, followed by Panavia SA, Panavia V5 and rodin bond and lastly Panavia V5 with clearfil with 6.9%. Panavia SA had 2.23% mixed failures, Panavia V5 and clearfil had 3.34% mixed failures, 1.12% for resicem cement, with no mixed failures for Panavia V5 group bonded with clearfil.

Table 15. Descriptive of failure mode after SBS test in different post treatment groups

		Post-treatment				Total	
		Control		T/C treated			
		N	%	N	%	N	%
Cohesive		39	21.79%	38	21.84%	77	21.81%
adh-cohesive		4	2.23%	2	1.15%	6	1.7%
Adhesive		136	75.98%	116	66.67%	252	71.39%
Total		179	50.71%	174	49.29%	353	100.0%
Chi-square	χ^2	27.16					
	P-value	<.0001*					

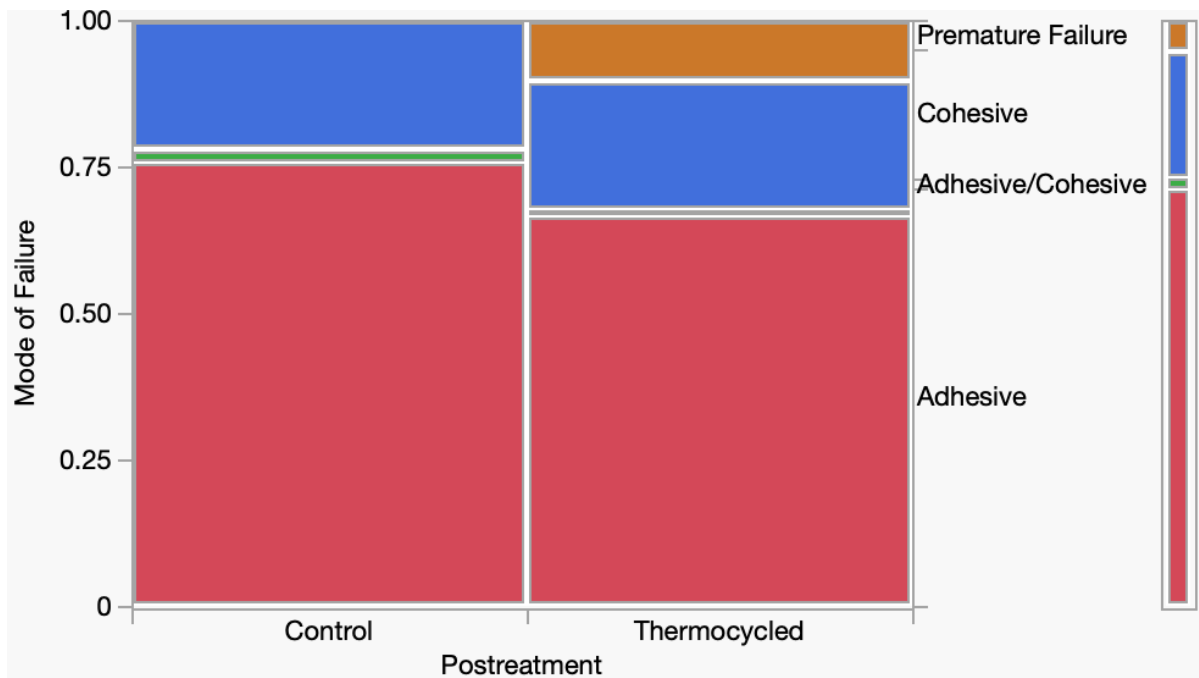


Figure 29. Mosaic plot of failure mode by post-treatment

Table 15 and Figure 29 show a significant difference between control groups and treated groups (thermocycled) regarding the failure mode in SBS. In control groups, 21.79% were a cohesive failure, 2.23% were adh-cohesive (mixed), and 75.98% were adhesive. In the treated groups, 21.84% were cohesive, 2 specimens were adh-cohesive (mixed), and 66.67% were adhesive failures.

Table 16. Descriptive of failure mode after SBS test in different material groups

SBS groups	Failure Type						Total	
	Cohesive		adh-cohesive		Adhesive		N	%
	N	%	N	%	N	%		
Layzir	0	0.0%	2	2.23%	83	93.26%	89	100.0%
Zirconia								
Pacdent	31	34.07%	1	1.10%	51	56.04%	91	100.0%
Sculpture 2								
Sprintray								
Ceramic	31	37.35%	3	3.61%	48	57.83%	83	100.0%
Crown								
Titan	15	16.67%	0	0.0%	70	77.78%	90	100.0%
Total	77	21.81%	6	1.70%	252	71.38%	353	100.0%
Chi-square	χ^2	56.24						
P-value	P-	<0.0001*						

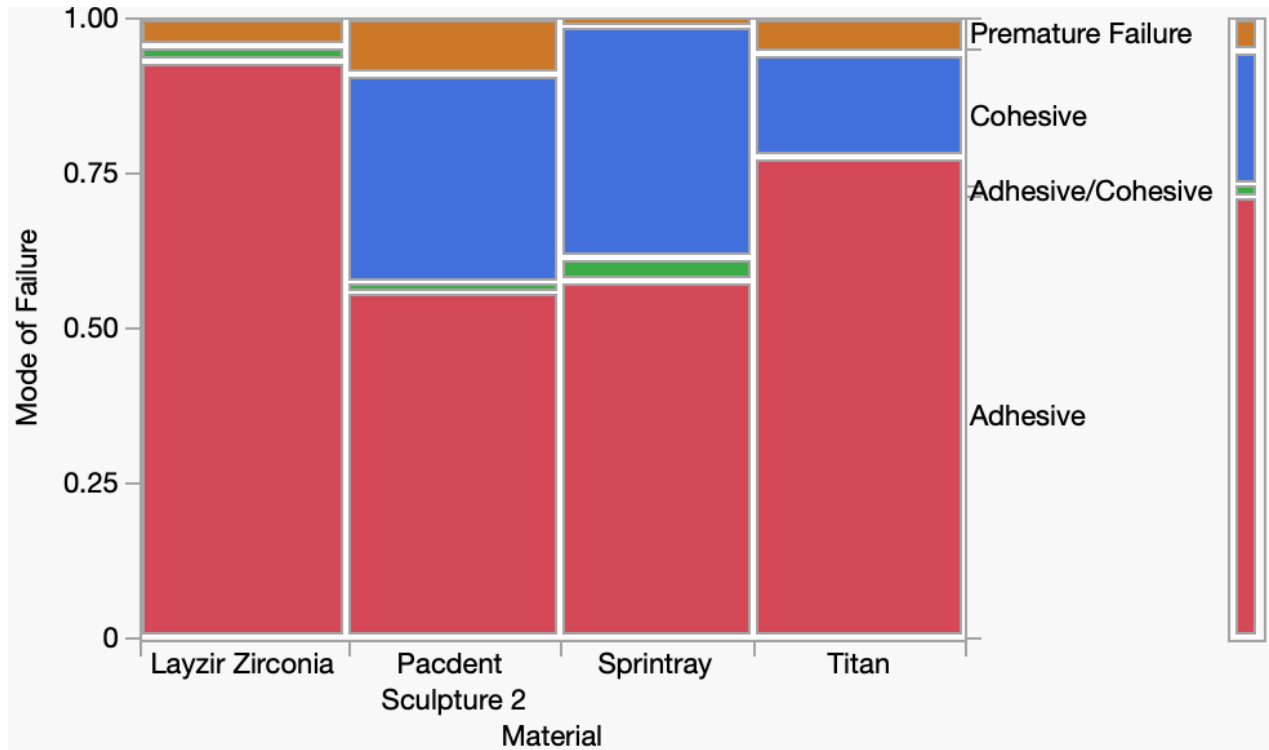


Figure 30. Mosaic plot of failure mode affected by substrate material

Table 16 and Figure 30 show a significant difference between groups regarding the failure mode, Layzir Zirconia groups showed 93.26% adhesive failure, with no cohesive failures. Pacdent Sculpture 2 showed 56.04% adhesive failures, with 34.07% cohesive failures. Sprinray ceramic crown showed 57.83% adhesive failures with 37.35% cohesive failures. Titan showed 71.38% adhesive failures with 21.81% cohesive failures.

Figure 32, and Figure 34 shows specimens with adhesive failures of different material and cement-bond combinations, examined using an optical microscope. Whereas Figure 33 and

Figure 35 shows cohesive failure of specimens of different material and cement-bond combinations.

3.3 Correlation of failure mode and shear bond strength

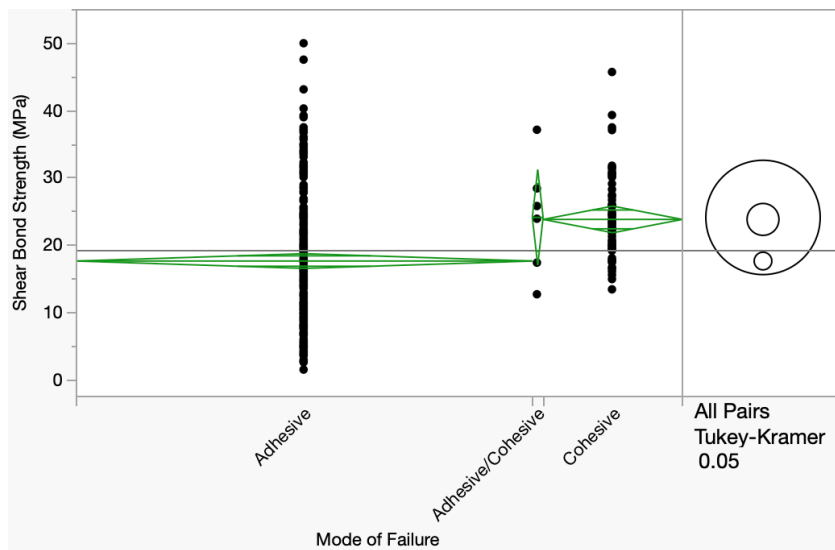


Figure 31. One-way analysis of shear bond strength MPa by mode of failure (adhesive, cohesive, mixed failure)

Table 17. One-way Anova and Tukey HSD test of SBS and mode of failure

Source	DF	Sum of square	Mean square	F ratio	Prob > F
Mode of failure	2	2400.45	1200.23	15.38	<.0001*
Error	332	25905.97	78.03		

C. Total	334	28306.42			
----------	-----	----------	--	--	--

Table 18. Connecting letters report for comparing SBS mean values and mode of failure using Tukey-Kramer HSD

Failure mode			Mean (MPa)
Mixed	A	B	24.17
Cohesive	A		23.87
Adhesive		B	17.69

Figure 31 shows statistically significant difference between adhesive and cohesive failures. It can also be seen that cohesive failure is significantly higher (P-value<0.0001) than adhesive failures in terms of SBS mean values.

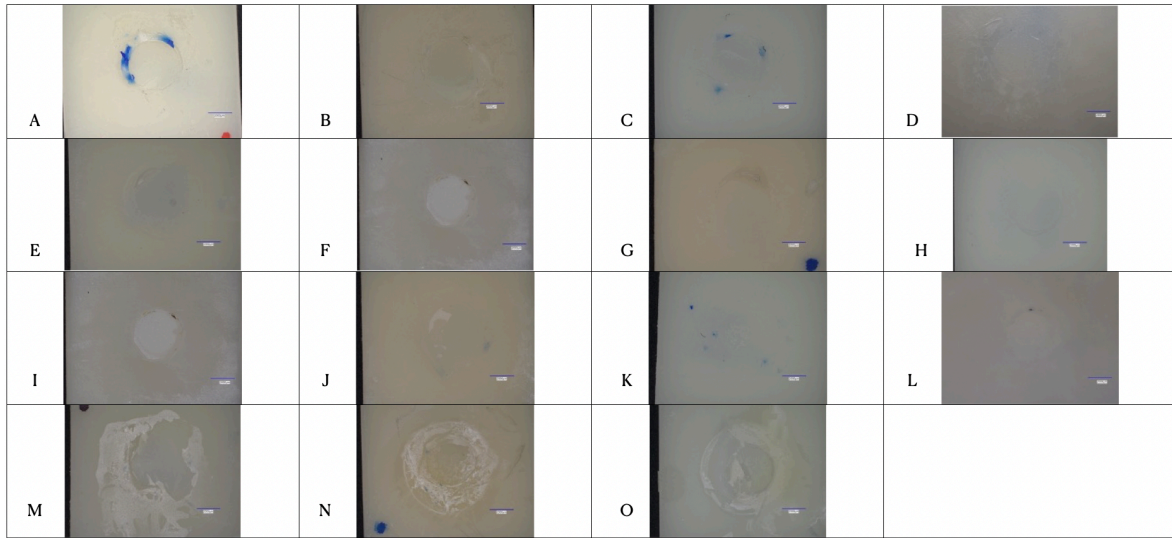


Figure 32. Adhesive failures shown in the failed SBS specimens

A.Pacdent Sculpture 2, Rodin Bond, Panavia V5, B.Sprintray, Rodin bond, Panavia V5, C.Titan, Rodin bond, Panavia V5, D.Zirconia, Rodin bond, Panavia v5, E. Pacdent, Clearfil, Panavia V5, F. Pacdent, Clearfil, Panavia v5, G. Sprintray, Clearfil, Panavia v5, H. Titan, Clearfil, Panavia v5, I. Pacdent, Clearfil, Panavia v5, J. Sprintray, Panavia SA, K. Titan, Panavia SA, L. Zirconia, Panavia SA, M. Pacdent, HC primer, Resicem EX, N. Sprintray, HC primer, Resicem EX, O. Titan, HC primer, Resicem EX

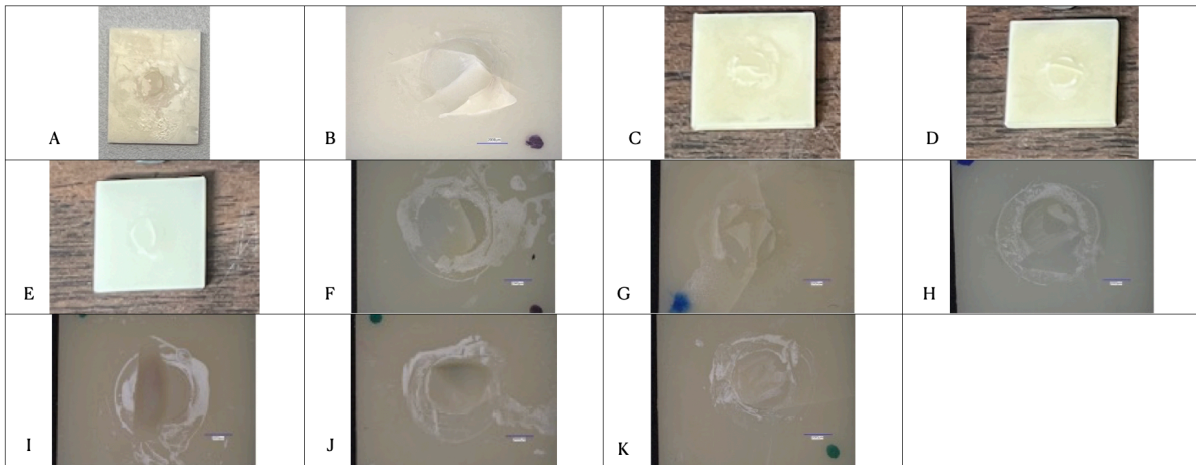


Figure 33. Cohesive and mixed failures among groups

A. Layzir Zirconia, Clearfil, Panavia V5, B. Pacdent, Rodin Bond, Panavia V5, C. Sprintray, Rodin Bond, Panavia v5, D. Sprintray Rodin Bond, Panavia v5, E. Titan, Rodin Bond, Panavia V5, F. Pacdent, HC Primer, Resicem EX, G. Sprintray, HC Primer, Resicem EX, H. Titan, HC Primer, Resicem EX, I. TC Sprintray, Clearfil, Panavia v5, J. TC Sprintray, Panavia SA, K. TC Sprintray, Panavia SA.

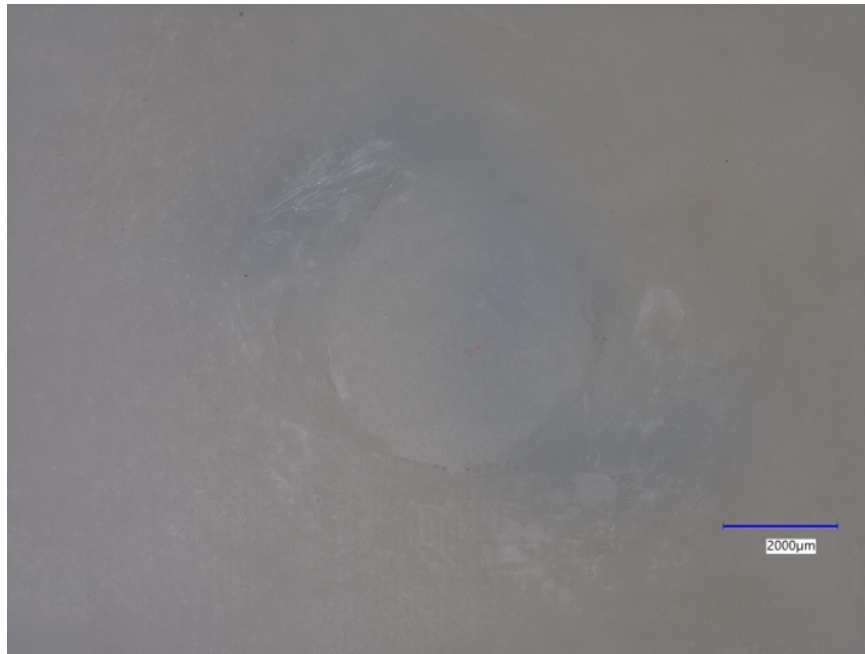


Figure 34. Adhesive failures shown in the failed SBS specimen (Layzir Zirconia, Rodin Bond, Panavia V5)



Figure 35. Cohesive failure shown in the failed SBS specimen (Pacdent, Rodin Bond, Panavia V5)

CHAPTER 4. DISCUSSION

4.1 Shear bond strength

This in vitro study measured the bonding of different cements and material combinations, and the effect of thermocycling on shear bond strength was also measured. Null hypotheses were rejected after significant differences in shear bond strength values were demonstrated in the current study. 3D printed resin materials have been commercially available recently, and there are limited published articles regarding mechanical properties. In most cases, only manufacturer data are available to compare with some of the materials in this study.

The overall objective of this in-vitro study was to measure bonding of multi and single step cements to printed resins and Layzir zirconia. The effect of different material combinations on shear bond strength was measured, and the effect of thermocycling on shear bond strength of different materials combinations was also measured.

In this in vitro study; the experimental specimens were standardized in terms of design, size, surface preparation, storage conditions and cementation load. Three types of resin cements were used: Panavia V5, Panavia SA, and Resicem EX. Four types of adhesive/primers were used: Rodin bond, Clearfil ceramic Primer Plus, HC primer and AZ primer (for resins and zirconia, respectively). In addition, thermal aging was conducted to assess the bond strength. Although clinical trials are the best way to assess dental materials, laboratory studies can offer awareness into the clinical outcome. The protocol in this study

is supposed to imitate clinical situations as it permits for more variable control, is less technique sensitive, and is somewhat inexpensive in comparison to clinical research.

Considering the shear bond strength (SBS); it is the most common test method for measuring the adhesive bond strength. The advantages of the SBS test are that it is easy to use and could signify strength in oral conditions of specimens. In the present study, SBS test was accomplished to evaluate the bond strength between different material combination, as it was regularly reported for the assessment of resin-based materials' adhesion ability. Moreover, this test needed simple preparation of specimens and could be performed easily. Numerous factors could influence the bonding success between materials and, in turn, the shear bond strength values. These factors include material surface topography, surface treatment before bonding, storage conditions, type of substrate, rate of load application and the adhesive system used (Ates et al, 2018).

The first aim of the study was to evaluate the effect of using different material combinations on shear bond strength. A significant difference was found between 3D printed resin groups compared to Layzir Zirconia group in shear bond strength (P-value = 0.0004) (Table 6) (Figure 21) (Table 8). This led to the rejection of the null hypothesis. The results of this study are consistent with the results of Ugur et al (2023) that found that the increase in the amount of inorganic filler in provided a favorable effect on durable adhesion in CAD/CAM ceramics.

The second aim of the study was to determine the effect of using different multi and single step adhesives on different material combinations. It was found that cement-bond has a statistically significant effect on SBS (P-value <0.0001). A significant

difference was found between Panavia SA cement compared to Panavia V5 and Resicem EX (P-value <.0001). This led to the rejection of the null hypothesis. When combining Panavia V5 with Clearfil ceramic primer plus which contain MDP, the shear bond strength of Panavia V5 to zirconia increased (Serichetaphongse et al, 2022). According to Serichetaphongse et al (2022), the use of MDP and phosphate monomer resin cement provided similar bond strength even after thermocycling.

Resin types of cement and primers containing 10-methacryloyloxydecyl dihydrogen phosphate (10-MDP) monomer have been thought of as the materials of choice because of the chemical interaction found between the hydroxyl groups of the zirconia ceramic and the phosphate ester monomer of the MDP-containing material. Resin luting types of cement like Panavia, and some primers such as CLEARFIL ceramic primer (Kuraray, Osaka, Japan) are representatives of this type of material.

A study conducted by Moradabadi et al. (2014) revealed that the main mechanism of zirconia core bonding to a dental resin agent is micromechanical retention, and the highest shear bond strengths were gained through an airborne-particle abrasion.

Numerous factors play a vital role in zirconia's bonding strength properties, for example, surface topography nature, type of surface treatment, and adhesive system used. Previous studies showed a considerable increase in air abraded SBS values comparative to untreated zirconia as a result of surface morphology changes. A basic surface treatment technique is sandblasting. Removing organic contaminants from the material's surface, permits higher roughness, creates a new and useful surface layer, and increases micromechanical interlocking of polymer-based dental materials.

The most important purpose of air abrasion is to increase resin-zirconia bond strength by enhancing surface roughness, cleaning, and activating the ceramic surface, specifically when combined with an adhesive monomer-containing primer such as 10-MDP (Takeuchi et al, 2010) (Yang et al, 2010) (Kern et al, 2009).

In this study, the choice of surface treatment and adhesive primer was based on study design, materials applied, instruction protocols for each material and previous studies employing a similar selection.

This study showed significantly lower shear bond strength mean values for Layzir Zirconia groups (16.18 MPa) as compared to resin material groups (18.9-20.4 MPa) (Table 8). These results show that all test results met the recommended values for clinical bonding (10-13 MPa for good clinical value) (Thurmond et al, 1994) (Heinz, et al, 2006). This could be attributed to the filler content in 3D printed resin materials, as it was found in a study done by Hagino et al (2023) that the bond strength of silane primer (Clearfil ceramic primer plus), and MMA containing primer (HC primer) increased as the filler content increased. It was also found that the MMA containing primer treatment was as effective as the silane treatment, even for resin blocks with a high filler content (Hagino et al, 2023)

In this in vitro study, half of SBS specimens (N=192) were aged consisting of 5000 thermal cycles (5/55 °C; dwell time, 30 s) thermocycling, which would be around 4-5 years of clinical use. In long-term probability, the influence of thermocycling on the SBS of different materials plays an important role, as intraoral thermal changes can be simply replicated by means of thermal cycling process. The results of the existing study revealed a significant difference between control and post-treatment in all groups, showing a

significant decrease in post-treatment SBS mean (14.2 MPa) over the control group (23.4 MPa) (P-value <.0001). This led to rejection of the null hypothesis.

The lowest shear bond strength mean values were recorded in Layzir Zirconia thermocycled groups, followed by Titan thermocycled groups (Table 12) (Table 6). It was also shown that premature failures presented in the thermocycled groups, with no premature failures in the control groups. The results of this study are supported in the literature, as thermal cycling was found to decrease the bonding strengths of cement (Nikitha et al, 2022). This can be due to the effect of water during thermal cycling, where it acts as plasticizer that might degrade the network of polymers. It can weaken the filler-polymer interface by damaging the silane-filler interface's chemical bonds and filler-particle surfaces. As a result, the interface bond strength will be influenced, and shear bond values will be reduced. An additional rationale for reducing the shear bond strength values can be due to differences in coefficient of thermal expansion between the frameworks and the rods (Ghavami-Lahiji et al, 2018).

The mode of failure is categorized as such: cohesive failure of the cement, adhesive, and mixed. Cohesive failure: approximately 90% or more of the residual luting cement remained on the stainless-steel rod. Adhesive failure: 25% or less of the cement residue remained on the stainless-steel rod. Mixed failure: the cement residue fell between the limits above.

For all SBS test groups, the fracture analysis revealed that the modes of failure were adhesive, cohesive, and mixed. In this study, it was shown that cohesive failure is

significantly higher than adhesive failures in terms of SBS mean values (Figure 31) (Table 17) (

Table 18). According to Lankes et al (2023), they stated that high number of cohesive fractures in the 3D printed material highlights the high bond strength. Therefore, the observed failure mode supports the results of the bond strength values obtained in this study.

In addition, at the time of the loading process, the frequency of mixed and cohesive failures may be attributed to the unequal distribution of stress at the bonding interface (Zhou et al, 2014). In PacDent Sculpture 2, and SprintRay groups, the mode of failure was cohesive and mixed failure (34%, and 35.37% respectively), and this can be due to high bond strength in the interface (Table 6) (Figure 30). Higher bond strength value and cohesive failures shown in Figure 30 and Table 6 for thermocycled SprintRay bonded with Clearfil and Panavia V5 and Panavia SA, and thermocycled PacDent bonded with Panavia SA can be attributed to the enhancement of bonding between composite resins and silane coupler or to the post curing of the bonding resin by heating at temperatures up to 60°C during the thermal cycling (Yoshida et al, 2001).

4.2 Limitations of this study

One such limitation is the lack of comprehensive data regarding the resin materials and adhesives/cements tested in the study, making it difficult to draw accurate

comparisons. It should also be noted that some resins and adhesives are relatively new to the market, and as such, there is a dearth of available studies aside from manufacturer data.

This in-vitro study did not reproduce the precise oral conditions while running the testing and thermal aging. In addition, the experiments were constructed in a dry environment without taking into account contamination with saliva or blood which could influence the bonding value and reduce the retention strength. Moreover, the quantity of cements used in the study was small (three types).

Clinical trials are essential to understand the actual performance of ceramics in the oral environment and the function of luting agents and surface treatments on their performance. Additional studies of long-term water storage and thermal cycling (TC) and additional numbers of cements are required to evaluate the stability of the resin bond when bonded with different material combination.

Moreover, the surface treatment used in this study was restricted to air-abrasion for zirconia and SprintRay Ceramic Crown group whereas other variety of treatments like plasma treatment (etching) or laser grooving may be favorable to visualize the effect on adhesion. Thermal aging was the only treatment used in this study, whereas cyclic fatigue may be a suitable selection for potential research and to assess the flexural strength and load to failure following the treatment for comparison reasons.

4.3 Recommendations for Future Studies

1. Additional study can be conducted using different adhesive and cements with the materials for example, Beautibond with Resicem ex.

2. Carry out an assessment of use of different adhesive systems on the shear bond strength in addition to mechanical properties.
3. Carry out an assessment of use of different surface treatment such as plasma, laser grooving, acid etching and different air abrasion pressure and study the effect on adhesion.

CHAPTER 5. CONCLUSION

Within the limitations of this in vitro study, the following conclusions can be drawn:

- 1- There was a significant difference in shear bond strength of printed resin groups SprintRay Ceramic crown (20.40 MPa), Rodin Titan (19.80 MPa), Pacdent Sculpture 2 (18.86 MPa), compared to Layzir Zirconia (16.18 MPa)
- 2- Layzir Zirconia groups showed a significant difference in shear bond strength values and were the lowest among all tested groups.
- 3- There was a statistically significant effect of cement-bond combinations on SBS values.
- 4- Panavia SA cement is significantly higher ($P\text{-value} < 0.0001$) than Panavia V5 bonded with Clearfil and Rodin bond, and Resicem cements.
- 5- Thermal aging significantly decreased the SBS values of thermocycled groups (14.74 MPa) compared to control groups (24.14 MPa).
- 6- Adhesive failure was the primary mode of failure among all SBS tested groups, Sprintray and Pacdent Sculpture 2 groups showed mixed failure (adhesive-cohesive).
- 7- Cohesive failures have a significantly higher SBS mean values (23.87 MPa) in comparison to adhesive failures (17.69 MPa). And can be associated with increasing shear bond strength.

CHAPTER 6. REFERENCES

1. Abduo, J. L. (2014). Trends in computer-aided manufacturing in prosthodontics: a review of the available streams. *International journal of dentistry*. doi:<https://doi.org/10.1155/2014/783948>.
2. Alex G. (2008). Preparing porcelain surfaces for optimal bonding. *Compendium of Continued Education in Dentistry*. 29(6):324-35; quiz 36.
3. Alhussain M (2024). Evaluation of the mechanical and physical properties for 3D printed material and machinable composite. *Boston University Henry M. Goldman School of Dental Medicine Thesis Master of Science in Dentistry*.
4. Alkandari A. (2023). Evaluation of the mechanical and physical properties of 3D printed resin materials. *Boston University Henry M. Goldman School of Dental Medicine Thesis Master of Science in Dentistry*.
5. Altan B, Cinar S, Tuncelli B. (2019). Evaluation of shear bond strength of zirconia-based monolithic CAD-CAM materials to resin cement after different surface treatments. *Nigerian Journal of Clinical Practice*. 22(11):1475-1482. doi:10.4103/njcp.njcp_157_19
6. Asmussen E. (1983) Factors affecting the color stability of restorative resins. *Acta Odontologica Scandinavica*. 41(1):11-8.
7. Asmussen E. (1983). Softening of BISGMA-based polymers by ethanol and by organic acids of plaque. *Scandinavian Journal of Dental Research*. 92(3):257-61.
8. Ates SM, Caglar I, Yesil Duymus Z. (2018). The effect of different surface pretreatments on the bond strength of veneering resin to polyetheretherketone. *Jornal of Adhesion Science and Technology*. 32(20):2220-2231. doi:10.1080/01694243.2018.1468534
9. Bagheri, A. &. (2019). Photopolymerization in 3D printing. *ACS Applied Polymer Materials Journal*. 1(4):593-611.
10. Blatz MB, Chiche G, Holst S, Sadan A. (2007). Influence of surface treatment and simulated aging on bond strengths of luting agents to zirconia. *Quintessence Int*. 38(9):745-53.

11. Blatz MB, Sadan A, Kern M (2003). Resin-ceramic bonding: a review of the literature. *Journal of Prosthetic Dentistry*. 89(3):268-74.
12. Blatz MB, Sadan A, Kern M. (2008). Resin-ceramic bonding: a review of the literature. *Journal of Prosthetic Dentistry*. 89(3):268-74.
13. Blatz MB, Sadan A, Martin J, Lang B. (2004). In vitro evaluation of shear bond strengths of resin to densely-sintered high-purity zirconium-oxide ceramic after long-term storage and thermal cycling. *Journal of Prosthetic Dentistry*. 91(4):356-62.
14. Burke FJ, Fleming GJ, Nathanson D, Marquis PM (2002). Are adhesive technologies needed to support ceramics? An assessment of the current evidence. *Journal of Adhesion Dentistry*. 4(1):7-22.
15. Casucci A, Mazzitelli C, Monticelli F, Toledano M, Osorio R, Osorio E. (2010). Morphological analysis of three zirconium oxide ceramics: Effect of surface treatments. *Dental Materials*. 26(8):751-60.
16. Casucci A, Monticelli F, Goracci C. (2011). Effect of surface pre-treatments on the zirconia ceramic-resin cement microtensile bond strength. *Dental Materials*. 27(10):1024-1030. doi:10.1016/j.dental.2011.07.002
17. Cavalcanti AN, Foxton RM, Watson TF, Oliveira MT, Giannini M, Marchi GM. (2009). Bond strength of resin cements to a zirconia ceramic with different surface treatments. *Operative Dentistry*. 34(3):280-7.
18. Chen, H. C. (2021). Comparison of flexural properties and cytotoxicity of interim materials printed from mono-LCD and DLP 3D printers. *The Journal of Prosthetic Dentistry*. 126(5): 703-708. doi:https://doi.org/10.1016/j.prosdent.2020.09.003.
19. Christensen GJ. (1993). The rise of resin for cementing restorations. *Journal of American Dental Association*. 124(10):104-5.
20. Davidowitz, G. &. (2011). The use of CAD/CAM in dentistry. *Dental Clinics*, 55(3), 559-570. doi:https://doi.org/10.1016/j.cden.2011.02.011.
21. Dong, T. W. (2020). Accuracy of different tooth surfaces on 3D printed dental models: Orthodontic perspective. *BMC Oral Health*, 1-8.
22. Edelhoff D, Ozcan M. (2007). To what extent does the longevity of fixed dental prostheses depend on the function of the cement? Working Group 4 materials: cementation. *Clinical Oral Implants Research*. 18(3):193-204.

23. Ferracane JL, Stansbury JW, Burke FJ. (2011). Self-adhesive resin cements - chemistry, properties and clinical considerations. *Journal of Oral Rehabilitation*. 38(4):295-314.
24. Ghavami-Lahiji M, Firouzmanesh M, Bagheri H, Jafarzadeh Kashi TS, Razazpour F, Behroozibakhsh M. (2018). The effect of thermocycling on the degree of conversion and mechanical properties of a microhybrid dental resin composite. *Restorative Dentistry and Endodontics*. 43(2):1-12. doi:10.5395/rde.2018.43.e26
25. Ha SR. (2015). Biomechanical three-dimensional finite element analysis of monolithic zirconia crown with different cement type. *Journal of Advanced Prosthodontics*. 7(6):475-83.
26. Hagino R, Mine A, Matsumoto M, Miura J, Yumitate M, Ban S, Ishida M, Takaishi M, Meerbeek B, Yatani H, Ishigaki S. (2023). *Journal of Prosthodontic Research*. https://doi.org/10.2186/jpr.JPR_D_22_00301.
27. Hartley, O. S. (2022). The Effect of Stacking on the Accuracy of 3D-Printed Full-Arch Dental Models. *Polymers*. 14(24), 5465. doi:https://www.mdpi.com/2073-4360/14/24/5465.
28. Hatzifotis M, Williams A, Muller M, Pegg S. (2004). Hydrofluoric acid burns. *Burns*. 30(2):156-9.
29. Heikkinen TT, Lassila LV, Matinlinna JP, Vallittu PK. (2007). Effect of operating air pressure on tribochemical silica-coating. *Acta Odontologica Scandinavica*. 65(4):241-8.
30. Heinz L, Leoffel O, Hammerle C., (2006). Effect of thermocycling on bond strength of luting cements to zirconia ceramic. *Dental Materials*. 22, pp: 195–200.
31. Huang, S. H. (2013). Additive manufacturing and its societal impact: a literature review. *The International journal of advanced manufacturing technology*. 1191-1203. doi:https://doi.org/10.1007/s00170-012-4558-5.
32. Inokoshi M, De Munck J, Minakuchi S, Van Meerbeek B. (2014). Meta-analysis of bonding effectiveness to zirconia ceramics. *Journal of Dental Research*. 93(4):329-334. doi:10.1177/0022034514524228
33. Javaid, M. &. (2019). Current status and applications of additive manufacturing in dentistry: A literature-based review. *Journal of oral biology and craniofacial research*, 9(3), 179-185. doi:https://doi.org/10.1016/j.jobcr.2019.04.004.

34. Jockusch, J. &. (2020). Additive manufacturing of dental polymers: An overview on processes, materials and applications. *Dental materials journal*. 39(3), 345- 354. Retrieved 06 01, 2023.
35. Jongsma L. Cementation in adhesive dentistry: the weakest link 2012.
36. Kelly JR, Denry I. (2008). Stabilized zirconia as a structural ceramic: an overview. *Dental Materials*. 24(3):289-98.
37. Kern M, Barloi A, Yang B. (2009). Surface conditioning influences zirconia ceramic bonding. *Journal of Dental Research*. 88:817–22. <https://doi.org/10.1177/0022034509340881>, PMID:19767578
38. Kessler, A. H. (2020). D printing in dentistry—State of the art. *Operative dentistry*, 45(1), 30-40. doi:<https://doi.org/10.2341/18-229-L>.
39. Kim, K. H. (2002). The effect of filler loading and morphology on the mechanical properties of contemporary composites. *The Journal of prosthetic dentistry*, 87(6), 642-649. doi:<https://doi.org/10.1067/mpr.2002.125179>.
40. Ko, J. B. (2021). Effect of build angle and layer height on the accuracy of 3-dimensional printed dental models. *American Journal of Orthodontics and Dentofacial Orthopedics*. 160(3), 451-458. doi:<https://doi.org/10.1016/j.ajodo.2020.11.039>.
41. Koizumi H, Nakayama D, Komine F, Blatz MB, Matsumura H. (2012). Bonding of resin-based luting cements to zirconia with and without the use of ceramic priming agents. *Journal of Adhesive Dentistry*. 14(4):385-92.
42. Kuraray Nritake Dental Inc. 2023. *Adhesive resin cement system Panavia V5. Instructions for use*. Retrieved from Kuraray Dental: <https://panaviacements.com/wp-content/uploads/2019/09/IFU-PANAVIA-V5.pdf>. Accessed on July. 30th. 2024.
43. Kuraray Nritake Dental Inc. 2023. *Self-adhesive resin cement system Panavia SA Cement Universal Instructions for use*. Retrieved from Kuraray Dental: https://panaviacements.com/wp-content/uploads/2019/09/panavia_sa_cement_universal_ifu.pdf. Accessed on July 21st. 2024
44. Lankes V, Reymus M, Leibermann A and Stawarczyk B. (2023). Bond strength between temporary 3D printable resin

- and conventional resin composite: influence of cleaning methods and air-abrasion parameters. *Clinical Oral Investigations*. 27:31–43.
45. Lung CY, Matinlinna JP. (2012). Aspects of silane coupling agents and surface conditioning in dentistry: an overview. *Dental Materials*. 28(5):467-77.
 46. McCabe JF, Walls A. Applied dental materials. 9th ed. Oxford, UK: Blackwell Pub.; 2008.
 47. Meyer JM, Cattani-Lorente MA, Dupuis V. (1998). Compomers: between glass-ionomer cements and composites. *Biomaterials*. 19(6):529-39.
 48. Mine, A., Kabetani, T., Kawaguchi-Uemura, A., Higashi, M., Tajiri, Y., Hagino, R., Imai, D., Yumitate, M., Ban, S., Matsumoto, M. and Yatani, H. (2019). Effectiveness of current adhesive systems when bonding to CAD/CAM indirect resin materials: A review of 32 publications. *The Japanese Dental Science Review*, [online] 55(1), pp.41–50. doi:<https://doi.org/10.1016/j.jdsr.2018.10.001>.
 49. Miyazaki T, Nakamura T, Matsumura H, Ban S, Kobayashi T. (2013). Current status of zirconia restoration. *Journal of Prosthodontic Research*. 57(4):236-261. doi:10.1016/j.jpor.2013.09.001
 50. Moon J-E, Kim S-H, Lee J-B, Han J-S, Yeo I-S, Ha S-R. (2016). Effects of airborne-particle abrasion protocol choice on the surface characteristics of monolithic zirconia materials and the shear bond strength of resin cement. *Ceramics International*. 42(1, Part B):1552-62.
 51. Nikitha, Thapaswini, Y., Chary, N.O.B.P., Pardeshi, K.V., Chitumalla, R. and Cherukuri, S.A. (2022). Effect of Thermocycling on Shear Bond Strength of PEEK—A Comparative Study of Resin Luting Cements: An In-Vitro Study. *Journal of Pharmacy & Bioallied Sciences*, [online] 14(Suppl 1), pp.S679–S682. doi:https://doi.org/10.4103/jpbs.jpbs_119_22.
 52. Noda M, Okuda Y, Tsuruki J, Minesaki Y, Takenouchi Y, Ban S. (2010). Surface damages of zirconia by Nd:YAG dental laser irradiation. *Dental Material Journal*. 29(5):536-41.
 53. Nulty, A. (2022). A comparison of trueness and precision of 12 3D printers used in dentistry. *British Dental Journal Open*, 14. doi:<https://doi.org/10.1038/s41405-022-00108-6>.

54. Oyagüe RC, Monticelli F, Toledano M, Osorio E, Ferrari M, Osorio R. (2009). Effect of water aging on microtensile bond strength of dual-cured resin cements to pre-treated sintered zirconium-oxide ceramics. *Dental Material*. 25(3):392-9.
55. Ozcan M, Allahbeickaraghi A, Dündar M. (2012). Possible hazardous effects of hydrofluoric acid and recommendations for treatment approach: a review. *Clinical Oral Investigation*. 16(1):15-23.
56. Ozcan M, Vallittu PK. (2003). Effect of surface conditioning methods on the bond strength of luting cement to ceramics. *Dental Material*. 19(8):725-31
57. Ozcan M. (2002). The use of chairside silica coating for different dental applications: a clinical report. *Journal of Prosthetic Dentistry*. 87(5):469-72.
58. PacDent. 2024. *Rodin Bond Safety Data Sheet*. [Brochure]. PacDent Inc. Retrieved from: <https://www.dhpsupply.com/msds/220-471101.pdf>
59. Perdigão, J. (2020). Current perspectives on dental adhesion: (1) Dentin adhesion not there yet. *Japanese Dental Science Review*. 56(1):190-207 [10.1016/j.jdsr.2020.08.004](https://doi.org/10.1016/j.jdsr.2020.08.004)
60. Pereira Lde L, Campos F, Dal Piva AM, Gondim LD, Souza RO, Özcan M. (2015). Can application of universal primers alone be a substitute for airborne-particle abrasion to improve adhesion of resin cement to zirconia? *Journal of Adhesive Dentistry*. 17(2):169-74.
61. Quan, H. Z. (2020). Photo-curing 3D printing technique and its challenges. *Bioactive materials*, 5(1), 110-115. doi:<https://doi.org/10.1016/j.bioactmat.2019.12.003>
62. Radovic I, Monticelli F, Goracci C, Vulicevic ZR, Ferrari M. (2008). Self-adhesive resin cements: a literature review. *Journal of Adhesive Dentistry*. 10(4):251-8.
63. Revilla-León, M. &. (2019). Additive manufacturing technologies used for processing polymers: current status and potential application in prosthetic dentistry. *Journal of Prosthodontics*, 28(2), 146-158. doi:10.1111/jopr.12801.
64. Rodin 3d Resins. 2023. *Rodin Sculpture 2.0 Instructions for use*. [Brochure]. Retrieved from: https://rodin-3d.com/instructions/IFU/Rodin-IFU_Sculpture-2-0.pdf. Accessed on July 14th. 2024

65. Rodin 3d Resins. 2023. *Rodin Titan Instructions for use*. [Brochure]. Retrieved from: https://rodin-3d.com/instructions/IFU/Rodin-Titan_IFU.pdf. Accessed on July 15th. 2024.
66. Rosenstiel SF, Land MF, Crispin BJ. (1998). Dental luting agents: A review of the current literature. *J Prosthet Dent*. 80(3):280-301.
67. Schweiger, J. E. (2021). 3D printing in digital prosthetic dentistry: an overview of recent developments in additive manufacturing. *Journal of Clinical Medicine*, 10(9), 2010. doi:<https://doi.org/10.3390/jcm10092010>.
68. Segarra M, Segarra A. 2015. *A Practical Clinical Guide to Resin Cements*. 1st Edition. Publisher: Springer.
69. Shofu inc. 2024. *AZ Primer Instructions for use*. [Brochure]. Shofu dental Corporation. Retrieved from shofu: <https://www.shofu.com/wp-content/uploads/AZ-Primer-IFU-ES-71626-03.pdf>. Accessed on June 18th. 2024.
70. Shofu inc. 2024. *Dental Adhesive Resin Cement Resicem Instructions for use*. [Brochure]. Shofu dental Corporation. Retrieved from Shofu: <https://www.shofu.com/wp-content/uploads/ResiCem-IFU-US-71255-03.pdf>. Accessed on June 17th. 2024.
71. Shofu inc. 2024. *HC Primer Instructions for use*. [Brochure]. Shofu dental Corporation. Retrieved from Shofu: <https://www.shofu.com/wp-content/uploads/HC-Primer-IFU-ES-71640-04.pdf>. Accessed on June 17th. 2024.
72. Sotov, A. K. (2021). LCD-SLA 3D printing of BaTiO₃ piezoelectric ceramics. *Ceramics International*, 47(21), 30358-30366. doi:<https://doi.org/10.1016/j.ceramint.2021.07.216>.
73. Spohr AM, Borges GA, Júnior LH, Mota EG, Oshima HM. (2008). Surface modification of In-Ceram Zirconia ceramic by Nd:YAG laser, Rocatec system, or aluminum oxide sandblasting and its bond strength to a resin cement. *Photomedicine and Laser Surgery*. 26(3):203-8.
74. Sprintray Inc. 2023. *Sprintray Ceramic Crown Instructions for use*. [Brochure]. Retrieved from: https://sprintray.com/oracle/uploads/2023/08/IFU-016_5-SprintRay-Ceramic-Crown-IFU.pdf. Accessed on Aug 5th. 2024.
75. Stansbury, J. W. (2016). 3D printing with polymers: Challenges among expanding options and opportunities. *Dental materials*, 32(1), 54-64. doi:<https://doi.org/10.1016/j.dental.2015.09.018>.

76. Sümer E, Değer Y. (2011). Contemporary Permanent Luting Agents Used in Dentistry: A Literature Review. *International Dental Research*. 11(1):26-3126.
77. Takeuchi K, Fujishima A, Manabe A, Kuriyama S, Hotta Y, Tamaki Y, et al. (2010). Combination treatment of tribochemical treatment and phosphoric acid ester monomer of zirconia ceramics enhances the bonding durability of resin-based luting cements. *Dental Materials Journal*. 29(3):316-23.
78. Tanaka R, Fujishima A, Shibata Y, Manabe A, Miyazaki T. (2008). Cooperation of phosphate monomer and silica modification on zirconia. *Journal of Dental Research*. 87(7):666-70.
79. Terry DA. (2004). Selecting a luting cement: part I. *Practical Procedures in Aesthetic Dentistry*. 16(10):718, 20.
80. Thompson JY, Stoner BR, Piascik JR, Smith R. (2011). Adhesion/cementation to zirconia and other non-silicate ceramics: where are we now? *Dental Materials*. 27(1):71-82.
81. Thurmond JW, Barkmeier WW, Wilwerding TM. (1994). Effect of porcelain surface treatments on bond strengths of composite resin bonded to porcelain. *Journal of Prosthetic Dentistry*. 72(4):355-9.
82. Tian, Y. C. (2021). A review of 3D printing in dentistry: Technologies, affecting factors, and applications. *Scanning*, doi:https://doi.org/10.1155%2F2021%2F9950131.
83. Tsolakis, I. A. (2022). Comparison in Terms of Accuracy between DLP and LCD Printing Technology for Dental Model Printing. *Dentistry Journal*. 10(10), 181. doi:https://doi.org/10.3390/dj10100181.
84. Tsuo Y, Yoshida K, Atsuta M. (2006). Effects of alumina-blasting and adhesive primers on bonding between resin luting agent and zirconia ceramics. *Dental Materials J*. 25(4):669-74.
85. Turkyilmaz, I. W. (2021). Tooth preparation, digital design and milling process considerations for CAD/CAM crowns: Understanding the transition from analog to digital workflow. *Journal of Dental Sciences*, 16(4), 1312-1314. doi:https://doi.org/10.1016%2Fj.jds.2021.04.005
86. Uğur, M., Kavut, İ., Tanrıkut, Ö.O. and Cengiz, Ö. (2023). Effect of ceramic primers with different chemical contents on the shear bond strength of CAD/CAM

ceramics with resin cement after thermal ageing. *BMC oral health*, [online] 23(1), p.210. doi:<https://doi.org/10.1186/s12903-023-02909-z>

87. Van Meerbeek, B., et al. (2003). "State of the art of self-etch adhesives." *Dental Materials* 19(6): 486-498.
88. www.sciencedirect.com. (n.d.). *Glass Ionomer - an overview | ScienceDirect Topics*. [online] Available at: <https://www.sciencedirect.com/topics/pharmacology-toxicology-and-pharmaceutical-science/glass-ionomer>.
89. Yang B, Barloi A, Kern M. (2010). Influence of air-abrasion on zirconia ceramic bonding using an adhesive composite resin. *Dental Materials*. 26(1):44-50.
90. Yoshida K, Kamada K, Atsuta M. (2001). Effects of two silane coupling agents, a bonding agent, and thermal cycling on the bond strength of a CAD/CAM composite material cemented with two resin luting agents. *The journal of prosthetic dentistry*. 85(2): 184-189.
91. Yun JY, Ha SR, Lee JB, Kim SH. (2010). Effect of sandblasting and various metal primers on the shear bond strength of resin cement to Y-TZP ceramic. *Dental Material*. 26(7):650-8.
92. Zhou L, Qian Y, Zhu Y, Liu H, Gan K, Guo J. (2014). The effect of different surface treatments on the bond strength of PEEK composite materials (DEMA-D-13-00481). *Dental Material*. 30(8): e209-e215. doi:10.1016/j.dental.2014.03.011.
93. Zhu, J. W. (2022). Recent advances in 3D printing for catalytic applications. *Chemical Engineering Journal*, 433(1), 134341. doi:<https://doi.org/10.1016/j.cej.2021.134341>
94. Zimmermann M, Ender A, Mehl A. (2020). Influence of CAD/CAM Fabrication and Sintering Procedures on the Fracture Load of Full-Contour Monolithic Zirconia Crowns as a Function of Material Thickness. *Operative Dentistry*. 45(2):219-226. doi:10.2341/19-086-L

CURRICULUM VITAE

